LARGE DEFORMATION ANALYSIS OF THERMO-ELASTIC CONTACT PROBLEMS

by

UTSA MAJUMDER

Department of Aerospace Engineering

Indian Institute of Technology, Kanpur

June, 2005

Certificate

This is to certify that the work contained in the thesis entitled *Large Deformation Analysis of Thermo-elastic Contact Problems* submitted by *Utsa Majumder* is carried out under my supervision. This work has not been submitted elsewhere for a degree.

C.S. Upadhyay

Dr. C.S. Upadhyay
Department of Aerospace Engineering
I.I.T. Kanpur
India

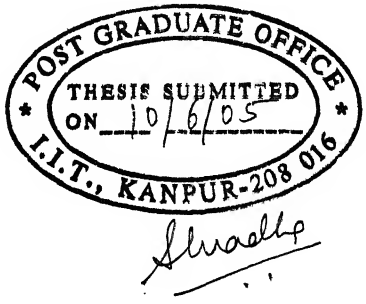

Dedicated to:

My Parents and Teachers

Acknowledgements

First of all, I would like to convey my gratitude to my thesis supervisor Dr. C.S. Upadhyay, whose able, professional and yet friendly guidance and support was with me for more than one year as a source of motivation. His interests and confidence in me were the underlying source of inspiration for this work.

Moreover, I am thankful to all my friends who made my stay at IIT Kanpur a memorable one. Specially, my days with Hall-7, E top members will be a sweet memory for the rest of my life. Some of them, like Shamik-da, Krishnendu, Anik, Soumya, Partha, were very friendly and helpful through out my program. I would also like to name some of my friends who are not in the institute now, and some seniors like Ashok, Pritam, Somnath, Abhijit-da, Sidhhartha-da, Sandip-da, Kaustubh-da, Rakesh-da, Kaushik-da, Debasis-da and many others who shared their happy moments with me.

I shall like to thank Abhijit-da specially for providing some helpful technical hints related to my work. Also the help, support and motivation from every person related to this work directly or indirectly, are gratefully acknowledged.

Utsa Majumder

June, 2005

Abstract

The present work is mainly targeted to develop an algorithm for total and updated Lagrangian formulations for large deformation dynamic thermoelastic problem with contact from their basic definitions using proper transformations and assumptions.

The main frame-work of this study is based on the Updated Lagrangian formulation and its application for some standard problems by coding it using Finite Element approximations. Updated Lagrangian method is developed on the incremental basis from the current configuration to the unknown deformed one. Related objective stress measures are formulated using the required incremental transformations. With proper approximations, the Jaumann-Zaremba objective stress increment rate is used for the computer program.

Thermal equations are considered to be decoupled from their elastic counterparts and are solved independently beforehand to generate required temperature fields and thermal stresses which is a input to the elastic problem.

Simple contact condition like sticking contact with a rigid wall is considered. The contact constraints are resolved into discrete form required for Finite Element Analysis using the Lagrangian multiplier method.

Also some work had been done on continuation methods and advanced solution procedure like the arc-length methods. The existing theories are revisited and a specific method, namely the cylindrical arc-length method, is incorporated into the static code to capture a few well known unstable phenomena.

Contents

List of Figures

List of Tables

List of symbols

Symbol Used	···	Meaning of the symbol
$\tilde{x}$	···	Generic spatial point
$\tilde{x}_t$	···	A spatial point at a generic time t
$\tilde{X}$	···	Generic material point
$\tilde{u}_t(\tilde{x})$	···	Displacement field at a spatial point $\tilde{x}$ at a generic time t
$\Delta\tilde{u}$	···	Increment in displacement $\tilde{u}$ from time t to $t + \Delta t$
$\delta\tilde{u}$	···	Virtual displacement field
$\tilde{v}$	···	Velocity field
m	···	Pointwise mass
$\mathcal{L}$	···	Linear momentum of a body
$\tilde{T}(\tilde{x}, \tilde{n}, t)$	···	Surface traction function at point $\tilde{x}$, with normal $\tilde{n}$ at time t
$\tilde{b}(\tilde{x}, t)$	···	Body force at a point $\tilde{x}$ at time t
$\tilde{f}_{ext}(\tilde{x}, t)$	···	External force at a point $\tilde{x}$ at time t
$\tilde{f}(., t)$	···	A mapping function which maps $\tilde{x}$ to $\mathcal{R}$
$\tilde{\tilde{F}}_t$	···	Deformation Gratient at time t
$\tilde{\tilde{G}}$	···	Incremental displacement gradient from time t to $t + \Delta t$
$\tilde{\tilde{\varepsilon}}$	···	General strain measure
$\tilde{\tilde{\epsilon}}$	···	Almansi strain
$\tilde{\tilde{\tau}}$	···	General stress measure
$\tilde{\tilde{\sigma}}_t$	···	Cauchy stress tensor at generic time t
$\theta(\tilde{x}, t)$	···	Temperature of a point $\tilde{x}$ at time t
$\Delta\theta$	···	Increment in temperature from time t to time $t + \Delta t$
$\delta\theta$	···	Virtual temperature field
s	···	Entropy of the thermoelastic system
ρ_t	···	Density at time t
k_i	···	Thermal heat condution coefficient in the i^{th} direction
α	···	Isotropic thermal strain coefficient
c	···	Coefficient of heat absorption
q^b	···	Heat generated pointwise inside the body
$\mathbf{C}_{ijkl}$	···	Fourth order material constant

E	$\cdots$	Young's modulus
ν	$\cdots$	Poisson's ratio
$\mathbb{W}(\tilde{\tilde{\varepsilon}})$	$\cdots$	Strain energy function for hyper-elastic materials
Π	$\cdots$	Potential energy
$\tilde{\tilde{L}}$	$\cdots$	Velocity gradient
$\tilde{\tilde{D}}$	$\cdots$	Deformation rate tensor (symm part of $\tilde{\tilde{F}}$)
$\tilde{\tilde{W}}$	$\cdots$	Spin tensor (skew part of $\tilde{\tilde{F}}$)
$\mathcal{B}_t$	$\cdots$	Domain of body in Eulerian space at a generic time t
$\partial\mathcal{B}_t$ or Γ_t	$\cdots$	Boundary of body in Eulerian space at a generic time t
$\tilde{n}_t$	$\cdots$	Normal on the boundary of a body at a generic time t
$\dot{q}$	$\cdots$	Spatial time darivative of the parameter q (scalor or tensor)
q'	$\cdots$	Material time darivative of the parameter q (scalor or tensor)
$\tilde{u}^e$	$\cdots$	Vector containing the values of displacements at the nodal points

Chapter 1

Introduction

The primary goal of the study is to understand the actual meaning of the still debatable terms - updated and total Lagrangian methods. An idea, clear to some extent, has been developed from the existing materials. The basic definitions of the processes are used to develop the corresponding balance laws. The resulting equilibrium equations are expressed in an incremental form. This use of incremental form introduces the requirement of the use of objective stress measures to confirm frame indifference of the physical parameters. The existing objective stress measures like Jaumann-Zaremba stress rate and Truesdell rates are shown as the special form of the objective stress increments and are used with proper approximations.

In this study, decoupled thermo-elastic problem is solved. By this approximation, first the temperature field in the body is obtained by solving the heat conduction problems,using finite elasticity formulation. This temperature field is then used to obtain the thermal loading on the structure. In the scope of this work, though the constitutive theories are deduced in a general manner, the balance equations for heat flux are considered to be decoupled from the elastic part while developing the computer code.

The contact problem, one of the most attractive and yet difficult one, is considered for a simple sticking contact with a rigid body. Basically, the challenging problem of multi-body deformable mechanics with contact search problem is reduced to a mere single body problem with pre-imposed constraints on certain degree of freedoms.

Also some continuation techniques are studied regarding the advanced solution methods. These limit point analyses are very good examples where the updated method has an positive advantage over the total Lagrangian method. Instead of handling the intricacies of the complex continuation techniques, rather a simple method like cylindrical arc-length method which is a readily programmable one, is introduced in the code.

Ultimately, for the dynamic analysis of the models, Newmark β integration scheme is used for the time integration part. Though this is an implicit time integration scheme, it shows some oscillations when implemented to the code. This phenomenon is also mentioned in some of the literatures. The oscillations resulting from the standard integration scheme proposed by Newmark has been damped out by introducing algorithmic damping.

1.1 Literature review

As the topic of the thesis was a classical one, many text books are available regarding the issues. Though some of them give conflicting definitions on updated Lagrangian method, overall they all focus on the same procedure and tactics.

Gurtin [1] and Malvern [2] has given a nice treatise on classical continuum mechanics which is essential for the understanding of the elementary kinematics of the deformable bodies. The basics of updated Lagrangian scheme are stated in Bathe [3] and Belytschko [4]. Both of them mentioned the updated and total Lagrangian approach as the extension of the same kind of analysis. Belytschko [4] has described the updated Lagrangian method to be the one where the measures of the physical quantities and the domain of the integral are taken about the Eulerian coordinate instead of the Lagrangian one used in total Lagrangian formulation and also showed the equivalence of the two formulations by proper coordinate transformation. But Bathe [3] has marked the difference between these two by the updation of the initial configuration used. According to him, in updated Lagrangian method, the initial configuration is updated continuously by one step to be used in the next step. The advantage of the updated Lagrangian method, as described here, lies in the predicting the actual path for large deformation problems (application of Taylor's series expansion is more valid as the total deformation path is divided into small parts) as well as the numerical advantages. Though Bathe, Ramm and Wilson [5] mentioned the incremental equations of motion, the expression of the conservation laws were in total or instantaneous form and hence, for the kind of transformation used, no objective increment in the stress tensor was done. Gadala and Wang [6] deduced an incremental approach for analyzing the kinematic behavior of deformable bodies which they described as the ALE (Arbitrary Lagrangian Eulerian) approach. This approach closely follows the incremental formulation used in this thesis. The concept of the intermediate reference frame used in the ALE formulation by Askes, Kuhl and Steinmann [7] is also very close to the intermediate reference frame at time t used in this analysis with the original frame at time 0 and current frame at time $t + \Delta t$. McMeeking and Rice [8] presented an Eulerian approach to tackle large elasto-plastic deformation problem which, when transformed to the reference configuration, produces the Lagrangian method.

Crisfield [9] has given some applications of the updated Lagrangian method. He also introduced some objective measures of stress increment rate [10] while treating large strains. The objectivity requirements for different kinematical quantities are mentioned in [1],[11] and [2]. Lecture notes on mechanics of solids of Brown University available from the web [12] have elaborately deduced the Oldroyd stress rate as a general objective rate for large deformation and large rotation and has shown that the other stress rates are special versions of the Oldroyd rate. Belytschko [4] also mentioned about the Jaumann, Truesdell and Green-Naghdi rates according to the constitutive equation used. With relevant assumptions, the Jaumann-Zaremba stress rate is used in the computer program as shown in [10].

The thermal conduction laws and governing equations for heat transfer are available in Bathe [3], Cook [13] and Haupt. Haupt [11] and Lubliner [14] also treated the constitutive assumptions for thermo-elasticity in a very general way. The constitutive assumptions mentioned in [1] and [2] are used to develop the constitutive relations for the analysis. In the code, isothermal material constants, given in

Lubliner [14], are used with standard numerical values.
The contact formulations used in this study are devoid of any kind of complexity. Rigorous study on the contact conditions for both small and large deformation is done by Wriggers [15] for sticking and slipping contact. Several schemes like Lagrangian multiplier method, penalty method, perturbed Lagrangian method etc. to handle the constraints are discussed thoroughly. The constraint conditions are discretized to fit the finite element analysis following the Lagrangian multiplier method and considering the contact to be a sticking one. Bathe [3], Crisfield [10] and Belytschko[4] have also given some brief review of the contact mechanics.
In this study, some work has been carried out on the advanced solution algorithms, mainly focusing on the continuation techniques. This methods generally guides the solution after a limit point is reached. A short textbook review of those methods are included in Crisfield [9, 10]. Similar works and their applications have been carried out by Ahmed and Xiao-Zu [16]. The cylindrical arc-length method introduced by Crisfield [9], is incorporated in the code and are applied to some standard structures with limit point loading.
For dynamic analysis of structures, implicit time integration scheme has been used. The schemes, explicit and implicit are available in Bathe [3] and Belytschko [4]. Newmark-β scheme, proposed originally by Newmark, is used in the computer program. It is simple to understand, use and apply in coding. But, the problem with this scheme is that, though it is said to be unconditionally stable, very often it shows an oscillation about the equilibrium values. Cook [13] mentioned the unstable or slow convergence behavior of Newmark integration scheme and has given some conditions on the time step length for the same to be unconditionally stable. This issue is also addressed by Mahato [17]. Some part of his work was regarding the stability of the Newmark-β scheme and he also introduced algorithmic damping by increasing the values of the Newmark constants. He mentioned the term *arrested instability* about this issue and also addressed slow convergence, though in [4] it is mentioned with respect to the explicit time integration scheme. In the current implementation, some oscillations are observed in the solution obtained from the program and these oscillations are damped out increasing the values of the Newmark constants to some higher numerical values. Further study using a more sophisticated time integration scheme, should be carried out in order to resolve this issue.

1.2 Structure of the thesis

In the current study, the work and simulations carried out have been addressed in an arranged manner. Chapter 2 covers the description of the different reference systems used in continuum mechanics, transformation between them, definitions of Eulerian, updated and total Lagrangian methods, basic conservation laws stemming out of the Reynold's transport theorem etc. The theory of objectivity has also been addressed in this section. This chapter is a short overview of the tools used in the whole study and are presented from a general point of view. The basic weak forms are developed and incremental techniques are described here.
In the next chapter, the focus is on the formulations done in this study. The continuum mechanics

laws and transformations presented in Chapter 2 are applied to the deformable solid body model to get the incremental version of the weak form of momentum balance. Using the laws of objectivity, the Jaumann-Zaremba rate, which is used in the current formulation while discretizing the equilibrium equations, is shown as a special case of the general objective stress rate with some assumptions.
The constitutive assumptions are also mentioned in this chapter and the constitutive laws are developed initially for hyper-elastic materials and then for thermoelastic materials using related potentials.
In Chapter 4, the contact constraints are formulated and discretized, Lagrangian multiplier technique is used and most of the formulations are done following Wriggers [15].
Chapter 5 contains overview of some continuation methods, namely the arc-length methods. Spherical, cylindrical and linearized arc length control techniques have been discussed under the light of generalized load-displacement control.
Chapter 6 is about discretizing the weak forms of conservation equations obtained in the previous chapters. Different strain displacement relations are formulated for Lagrangian shape functions. Newmark-β time integration scheme is used to modify the differential form into an algebraic equation.
Chapter 7 contains the results obtained from some simulations done using the computer program and their comparison with existing commercial codes and/or strength of material formulation. Mainly different static analyses are emphasized in the chapter. The issue of numerical oscillation for dynamic problems are also addressed briefly.

Chapter 2

Preliminaries of Continuum Mechanics

2.1 Kinematics

The target of this chapter is to focus on the tools used to analyze the systems under consideration. For kinematic systems, the basic laws are governed by continuum mechanics. The laws of nature here means the balance laws that the body must obey, namely, the continuity equation, conservation of linear and angular momentum and conservation of energy. In continuum mechanics formulations, generally two coordinate systems are used to completely describe the kinematics of a body as shown in Figure 2.1 for the convenience of the analysis [1]. The space fixed (with respect to the stars) coordinate system

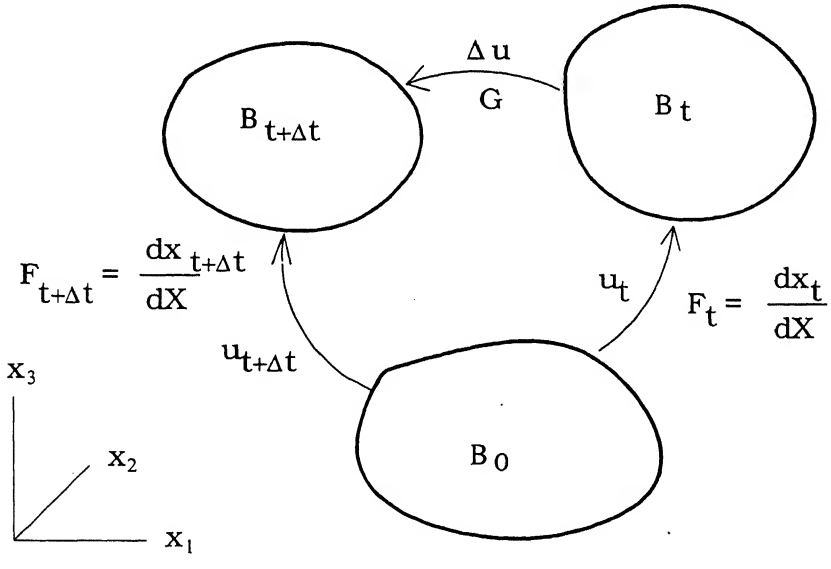

Figure 2.1: Reference, undeformed and deformed coordinate systems

is referred as the Eulerian or the spatial coordinate system and the one moving fixed with the body (or sometimes fixed with respect to some intermediate position) is called the Lagrangian or the material one. The governing laws of mechanics are written with respect to any one of these two reference systems. And correspondingly the type of the analysis changes. There are mainly two types of analysis

done in mechanics, Eulerian or spatial formulation and Lagrangian or material formulation. These two different formulations are just the different representation of the same balance laws with respect to the two different coordinate systems mentioned above.
In Eulerian or spatial formulation, the equilibrium equations are written with respect to the spatial coordinate system. The discretization is also done in the Eulerian coordinate. And for Eulerian finite element formulation, spatially fixed meshes are used. In contrast with this, in Lagrangian formulation, the equations are referred with respect to a material fixed coordinate. The basic idea of Lagrangian formulation is to freeze the reference coordinate system in time. For static problems, it is frozen to some virtual time step. Updated and total Lagrangian methods only differ in the regard of fixing the coordinate to a different time step [3].

2.2 Transformation between the two coordinate systems

The domain of the body in Euclidean space, $\mathcal{B}_t$ is property by which the bodies are referred from both material and spatial configuration. As shown in Figure 2.2, let us assume that the material coordinate of the body occupying the domain $\mathcal{B}_t$ is expressed by $\tilde{X}$ and the corresponding spatial coordinate for it is $\tilde{x}$.

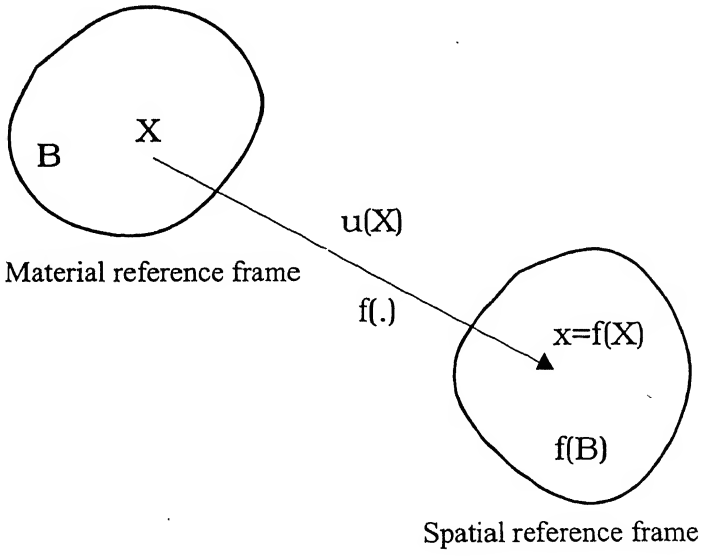

Figure 2.2: Transformation from material to spatial coordinate

From the basics of continuum mechanics, the spatial description of the body is a mapping $\tilde{f}$ of the material coordinate (and vice-versa) as:

$$\tilde{x} = \tilde{f}(\tilde{X}) \tag{2.2.1}$$

The expression $det\nabla\tilde{f}$ represents the local point-wise volume after deformation. And $\tilde{f}$ is assumed to

be a one-to-one mapping of the points $\tilde{X}$, it implies that the body cannot penetrate itself [1]. So,

$$det\nabla\tilde{f} > 0$$

The vector $\tilde{u}(\tilde{X})$ is the displacement between two generic points in the spatial and the material references.

$$\tilde{f}(X) = \tilde{X} + \tilde{u}(\tilde{X})$$

The tensor quantity, defined point-wise,

$$\begin{aligned}\tilde{\tilde{F}} &= \nabla\tilde{f}(\tilde{X}) \\ &= \frac{\partial\tilde{x}}{\partial\tilde{X}}\end{aligned}$$

is called the deformation gradient tensor [1]. As $det\nabla\tilde{f} > 0$, deformation gradient $\tilde{\tilde{F}}$ is a positive definite tensor. Deformation gradient may be considered as a measure of deformation or strain as $d\tilde{x} = \tilde{\tilde{F}}d\tilde{X}$

$$\begin{aligned}\tilde{\tilde{F}} &= \frac{\partial\tilde{x}}{\partial\tilde{X}} \\ &= \frac{\partial\tilde{f}(\tilde{X})}{\partial\tilde{X}} \\ &= \frac{\partial}{\partial\tilde{X}}(\tilde{X} + \tilde{u}) \\ &= \tilde{\tilde{I}} + \frac{\partial\tilde{u}}{\partial\tilde{X}}\end{aligned}$$

Mathematically, the deformation gradient is the Jacobian matrix of the motion of the body $\tilde{x}(\tilde{X}, t)$ [4]. It includes both rigid rotation and stretch. The total deformation may be considered as a rigid rotation operating on a stretch or vise-versa. Hence, polar decomposition may be used to find out the stretch part separately from the rigid rotation, which causes no strain with respect to the material reference frame[1].

$$\begin{aligned}\tilde{\tilde{F}} &= \tilde{\tilde{R}}\tilde{\tilde{U}} \text{ (Right polar decomposition)} \\ &= \tilde{\tilde{V}}\tilde{\tilde{R}} \text{ (Left polar decomposition)}\end{aligned}$$

where, $\tilde{\tilde{R}}$ is the rigid rotation tensor, $\tilde{\tilde{U}}$ and $\tilde{\tilde{V}}$ are the right and left stretch tensor respectively.
As $\tilde{\tilde{R}}$ is an orthogonal tensor,the *Right Cauchy-Green Strain tensor* and the *Left Cauchy-Green Strain tensor* is defined as:

are

$$\text{Right Cauchy-Green strain tensor: } \tilde{\tilde{C}} = \tilde{\tilde{U}}^2 = \tilde{\tilde{F}}^T \tilde{\tilde{F}}$$

$$\text{Right Cauchy-Green strain tensor: } \tilde{\tilde{B}} = \tilde{\tilde{V}}^2 = \tilde{\tilde{F}} \tilde{\tilde{F}}^T$$

Hence, the expressions for right and left Cauchy-Green strain can be derived as [1]

$$\begin{aligned}
\tilde{\tilde{C}} &= \tilde{\tilde{F}}^T \tilde{\tilde{F}} \\
&= (\tilde{\tilde{I}} + \frac{\partial \tilde{u}}{\partial \tilde{\tilde{X}}})^T (\tilde{\tilde{I}} + \frac{\partial \tilde{u}}{\partial \tilde{\tilde{X}}}) \\
&= \tilde{\tilde{I}} + \frac{\partial \tilde{u}}{\partial \tilde{\tilde{X}}} + (\frac{\partial \tilde{u}}{\partial \tilde{\tilde{X}}})^T + (\frac{\partial \tilde{u}}{\partial \tilde{\tilde{X}}})^T (\frac{\partial \tilde{u}}{\partial \tilde{\tilde{X}}}) \\
\text{And, } \tilde{\tilde{B}} &= \tilde{\tilde{F}} \tilde{\tilde{F}}^T \\
&= (\tilde{\tilde{I}} + \frac{\partial \tilde{u}}{\partial \tilde{\tilde{X}}})(\tilde{\tilde{I}} + \frac{\partial \tilde{u}}{\partial \tilde{\tilde{X}}})^T \\
&= \tilde{\tilde{I}} + \frac{\partial \tilde{u}}{\partial \tilde{\tilde{X}}} + (\frac{\partial \tilde{u}}{\partial \tilde{\tilde{X}}})^T + (\frac{\partial \tilde{u}}{\partial \tilde{\tilde{X}}})(\frac{\partial \tilde{u}}{\partial \tilde{\tilde{X}}})^T
\end{aligned}$$

The tensors $\tilde{\tilde{U}}$ and $\tilde{\tilde{V}}$ are similar, where $\tilde{\tilde{C}}$ and $\tilde{\tilde{B}}$ are also similar as:

$$\tilde{\tilde{V}} = \tilde{\tilde{R}} \tilde{\tilde{U}} \tilde{\tilde{R}}^T$$

$$\text{And, } \tilde{\tilde{B}} = \tilde{\tilde{R}} \tilde{\tilde{C}} \tilde{\tilde{R}}^T$$

where $\tilde{\tilde{R}}$ is an orthogonal matrix such that $\tilde{\tilde{R}}^{-1} = \tilde{\tilde{R}}^T$.

2.3 Balance Laws

2.3.1 Reynold's transportation theorem

The balance laws of continuum mechanics, or the conservation laws, are all branching out of the transportation theorem [11, 1]. Transportation theorem is basically a balance relation for an open system. The general statement of the Reynold's transportation theorem is as follows:
Let Φ be a smooth spatial field, and assume that Φ is either vector valued or scaler valued. Then for any part $\mathcal{B}_t$ and time t,

$$\begin{aligned}
\frac{d}{dt} \int_{\mathcal{B}_t} \Phi d\Omega &= \int_{\mathcal{B}_t} \left(\dot{\Phi} + \Phi div_{\tilde{x}} \, \tilde{v} \right) d\Omega \\
\frac{d}{dt} \int_{\mathcal{B}_t} \Phi d\Omega &= \int_{\mathcal{B}_t} \Phi' d\Omega + \int_{\partial \mathcal{B}_t} \Phi \tilde{v} \cdot \tilde{n} dS
\end{aligned} \tag{2.3.1}$$

Proof of Equation 2.3.1 is available in Gurtin [1] and Haupt [11]. This famous equation is basically the origin of all the balance laws of nature. A general open system is shown in Figure 2.3. The region

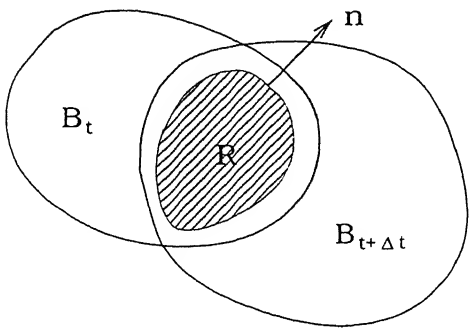

Figure 2.3: Control volume for time window Δt

$\mathcal{R}$ is the region under consideration for control volume analysis. For control mass analysis, which is followed in this section to get the corresponding conservation laws, $\mathcal{R}$ is equivalent to $\mathcal{B}_t$ at time t and to $\mathcal{B}_{t+\Delta t}$ at time $t + \Delta t$.

2.3.2 Continuity equation

The most important property of the bodies those are defined in the Eulerian space, is the matter contained in that space of the body $\mathcal{B}$ or in other words, mass. Mass of a body is defined as:

$$\begin{aligned} m(\tilde{X}) &= \int_{\mathcal{B}_t} dm \\ &= \int_{\mathcal{B}_t} \rho_t d\Omega \end{aligned}$$

Using Reynold's transport theorem,

$$\begin{aligned} \frac{d}{dt}m &= \frac{d}{dt}\int_{\mathcal{B}_t} \rho_t d\Omega \\ &= \int_{\mathcal{B}_t} \rho_t' d\Omega + \int_{\partial\mathcal{B}_t} \rho_t \tilde{v} \cdot \tilde{n} dS \end{aligned}$$

The term $\int_{\partial\mathcal{B}_t} \rho_t \tilde{v} \cdot \tilde{n} dS$ is a surface term representing the out flux of mass through the surface. But as $\mathcal{B}_t$ defines the body as a whole, this term is zero. Hence,

$$\begin{aligned} \frac{d}{dt}m &= \int_{\mathcal{B}_t} \rho_t' d\Omega \\ \Rightarrow \int_{\mathcal{B}_t} \rho_t d\Omega &= \int_{\mathcal{B}_0} \rho_0 d\Omega \end{aligned}$$

Now, if the deformation can be represented as a mapping $\tilde{f}$ and its gradient $\tilde{\tilde{F}} = \nabla \tilde{f}$ then, transforming domain of integration of L.H.S to $\mathcal{B}_0$ [1],

$$\int_{\mathcal{B}_0} det\left(\tilde{\tilde{F}}(\tilde{X})\right) \rho_t(\tilde{x}(\tilde{X}))d\Omega = \int_{\mathcal{B}_0} \rho_0(\tilde{X})d\Omega$$

Hence, the continuity (of mass) equation turns out to be:

$$det\left(\tilde{\tilde{F}}(\tilde{X})\right) \rho_t(\tilde{x}) = \rho_0(\tilde{X}) \tag{2.3.2}$$

Let Φ be a continuous spatial scaler field. Then, for any given body $\mathcal{B}_t$,

$$\begin{aligned}\int_{\mathcal{B}_t} \Phi(\tilde{x})\rho_t(\tilde{x})d\Omega &= \int_{\mathcal{B}_0} \Phi(\tilde{X})det(\tilde{\tilde{F}})\rho_t(\tilde{X})d\Omega \\ &= \int_{\mathcal{B}_0} \Phi(\tilde{X})\rho_0(\tilde{X})d\Omega\end{aligned}$$

So, as a point-wise statement, it can be written that,

$$\int_{\mathcal{B}_t} \Phi(\tilde{x})\rho_t(\tilde{x})d\Omega = \int_{\mathcal{B}_0} \Phi(\tilde{X})\rho_0(\tilde{x})d\Omega \tag{2.3.3}$$

2.3.3 Momentum balance

The mechanical motions of a body is governed generally by the external causes named "Force". In this study, the forces may be categorized mainly as:
(i) Contact forces between different parts of the body or the internal forces,
(ii) Contact forces exerted on the boundary of the body by the environment or external surface forces, and
(iii) Forces exerted on the volume of the body by the environment or external body forces.
The most important axiom in mechanics to describe the balance of momentum is *Cauchy's hypothesis*. This axiom assumes that there exists a surface force density function $\tilde{\mathbf{T}}(\tilde{\mathbf{x}}, \mathbf{t})$ for each unit normal vector $\tilde{n}$ and every $(\tilde{\mathbf{x}}, \mathbf{t})$ on the boundary $\partial\mathcal{B}_t$ as shown in Figure 2.4 [1].

This contact force is often referenced as the traction force. For the whole boundary $\partial\mathcal{B}_t$, the total traction force is

$$\int_{\partial\mathcal{B}_t} \tilde{T}(\tilde{n})dS$$

The sum of the body force applied by the environment on the body can be expressed as

$$\int_{\mathcal{B}_t} \tilde{b}d\Omega$$

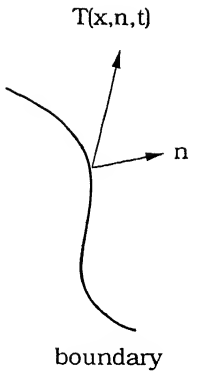

Figure 2.4: Surface force density function

Hence, the statement of the balance of linear momentum becomes:

$$\text{Total external force, } \tilde{f}_{ext}(\tilde{X},t) = \int_{\partial\mathcal{B}_t} \tilde{T}(\tilde{n})dS + \int_{\mathcal{B}_t} \tilde{b}d\Omega \tag{2.3.4}$$

By Newton's second law, if the linear momentum of the body is $\tilde{\mathcal{L}}$, then

$$\tilde{f}_{ext} = \frac{d\tilde{\mathcal{L}}}{dt} \tag{2.3.5}$$

And by Reynold's transport theorem,

$$\begin{aligned}\frac{d\tilde{\mathcal{L}}}{dt} &= \frac{d}{dt}\int_{\mathcal{B}_t} \rho\tilde{v}d\Omega \\ &= \int_{\mathcal{B}_t} \frac{d}{dt}(\rho\tilde{v})d\Omega + \int_{\partial\mathcal{B}_t} (\rho\tilde{v})\tilde{v}\cdot\tilde{n}dS \\ &= \int_{\mathcal{B}_t} \rho\dot{\tilde{v}}d\Omega + \int_{\mathcal{B}_t} \tilde{v}\dot{\rho}d\Omega\end{aligned}$$

as $\tilde{v}\cdot\tilde{n}$ is a measure of flux through the boundary $\partial\mathcal{B}_t$ and is zero for control mass formulation. Hence,

$$\frac{d\tilde{\mathcal{L}}}{dt} = m\ddot{\tilde{u}} + \dot{m}\dot{\tilde{u}} = \tilde{f}_{ext} \tag{2.3.6}$$

From Equation 2.3.4 and Equation 2.3.6, as the mass of the system is time independent, the force balance equations turns out to be

$$\int_{\partial\mathcal{B}_t} \tilde{T}(\tilde{n})dS + \int_{\mathcal{B}_t} \tilde{b}d\Omega = \int_{\mathcal{B}_t} \rho\ddot{\tilde{u}}d\Omega \ \ (= m\ddot{\tilde{u}}) \tag{2.3.7}$$

Cauchy's theorem (existence of stress): [1]
This theorem defines a spatial tensor quantity $\tilde{\sigma}$, called the Cauchy stress tensor. The existence of the stress tensor is a necessary and sufficient condition that the momentum balance equation should satisfy.

The statement of the theorem is:
(i) For each unit normal $\tilde{n}$, $\exists$ a tensor $\tilde{\tilde{\sigma}}$ such that, $\tilde{T}(\tilde{n}) = \tilde{\tilde{\sigma}}\tilde{n}$
(ii) $\tilde{\tilde{\sigma}}$ is symmetric, and
(iii) $\tilde{\tilde{\sigma}}$ satisfies the equation of motion

$$div_{\tilde{x}}\tilde{\tilde{\sigma}} + \tilde{b} = \rho\ddot{\tilde{u}} \tag{2.3.8}$$

The last statement is a point-wise statement of momentum balance and can be derived by putting the expression of $\tilde{\tilde{\sigma}}$ from statement (i) in Equation 2.3.7 and using Gauss divergence theorem.

2.3.4 Theorem of virtual work

Theorem of virtual work (or theorem of virtual power for the corresponding rate form) is the direct outcome of the momentum balance. A kinematically admissible (obeying the essential boundary condition) virtual displacement function $\delta\tilde{u}$ is assumed from the space all possible displacement fields of the body. The point-wise momentum balance equation (Equation 2.3.8) is multiplied and integrated over the whole domain to get the balance of virtual power.

$$\int_{\mathcal{B}_t} [div_{\tilde{x}}\tilde{\tilde{\sigma}} + \tilde{b}] \cdot \delta\tilde{u} d\Omega = \int_{\mathcal{B}_t} \rho\ddot{\tilde{u}} \cdot \delta\tilde{u} d\Omega$$

$$\text{or, } \int_{\mathcal{B}_t} div_{\tilde{x}}\left(\tilde{\tilde{\sigma}}\right) \cdot \delta\tilde{u} d\Omega + \int_{\mathcal{B}_t} \rho\tilde{b} \cdot \delta\tilde{u} d\Omega = \int_{\mathcal{B}_t} \ddot{\tilde{u}} \cdot \delta\tilde{u} d\Omega$$

using integration by parts,

$$\text{or, } \int_{\mathcal{B}_t} [div_{\tilde{x}}\left(\tilde{\tilde{\sigma}}\delta\tilde{u}\right) - \tilde{\tilde{\sigma}} : grad_{\tilde{x}}\delta\tilde{u}] d\Omega + \int_{\mathcal{B}_t} \rho\tilde{b} \cdot \delta\tilde{u} d\Omega = \int_{\mathcal{B}_t} \rho\ddot{\tilde{u}} \cdot \delta\tilde{u} d\Omega$$

using Gauss divergence theorem,

$$\int_{\partial\mathcal{B}_t} \tilde{\tilde{\sigma}}\delta\tilde{u} \cdot \tilde{n} dS - \int_{\mathcal{B}_t} \tilde{\tilde{\sigma}} : grad_{\tilde{x}}\delta\tilde{u} d\Omega + \int_{\mathcal{B}_t} \rho\tilde{b} \cdot \delta\tilde{u} d\Omega = \int_{\mathcal{B}_t} \rho\ddot{\tilde{u}} \cdot \delta\tilde{u} d\Omega$$

using statement (i) of Cauchy's theorem,

$$\int_{\partial\mathcal{B}_t} \tilde{T} \cdot \delta\tilde{u} dS - \int_{\mathcal{B}_t} \tilde{\tilde{\sigma}} : grad_{\tilde{x}}\delta\tilde{u} d\Omega + \int_{\mathcal{B}_t} \rho\tilde{b} \cdot \delta\tilde{u} d\Omega = \int_{\mathcal{B}_t} \rho\ddot{\tilde{u}} \cdot \delta\tilde{u} d\Omega$$

So, the theorem of virtual work or the weak form of the momentum balance equation in the deformed coordinate is:

$$\int_{\mathcal{B}_t} \rho\ddot{\tilde{u}} \cdot \delta\tilde{u} d\Omega + \int_{\mathcal{B}_t} \tilde{\tilde{\sigma}} : grad_{\tilde{x}}\delta\tilde{u} d\Omega - \int_{\mathcal{B}_t} \rho\tilde{b} \cdot \delta\tilde{u} d\Omega - \int_{\partial\mathcal{B}_t} \tilde{T} \cdot \delta\tilde{u} dS = 0 \tag{2.3.9}$$

2.3.5 Balance of Heat Flux

The governing heat conduction equation is build over the assumption that the material under consideration follows the **Fourier's Law** of heat conduction. Then for the heat flux equilibrium for any internal

point of the body [13, 3]

$$\frac{\partial}{\partial x_1}\left(k_{x_1}\frac{\partial\theta}{\partial x_1}\right)+\frac{\partial}{\partial x_2}\left(k_{x_2}\frac{\partial\theta}{\partial x_2}\right)+\frac{\partial}{\partial x_3}\left(k_{x_3}\frac{\partial\theta}{\partial x_3}\right)+q^b-c\rho\frac{d\theta}{dt}=0 \tag{2.3.10}$$

Assuming an admissible temperature field $\delta\theta$, the theorem of virtual work done by the heat flux can be derived as:

$$\int_{\mathcal{B}_t}[\frac{\partial}{\partial x_1}\left(k_{x_1}\frac{\partial\theta}{\partial x_1}\right)+\frac{\partial}{\partial x_2}\left(k_{x_2}\frac{\partial\theta}{\partial x_2}\right)+\frac{\partial}{\partial x_3}\left(k_{x_3}\frac{\partial\theta}{\partial x_3}\right)+q^b-c\rho\frac{d\theta}{dt}]\delta\theta d\Omega=0$$
$$\Rightarrow\int_{\mathcal{B}_t}(k_i\theta_{,i})_{,i}d\Omega+\int_{\mathcal{B}_t}q^b\delta\theta d\Omega-\int_{\mathcal{B}_t}c\rho\frac{d\theta}{dt}\delta\theta d\Omega=0$$

Hence, the weak form turns out to be

$$\int_{\partial\mathcal{B}_t}[\delta\theta(k_i\theta_{,i})]n_i dS-\int_{\mathcal{B}_t}(K_i\theta_{,i})\delta\theta_{,i}d\Omega+\int_{\mathcal{B}_t}q^b\delta\theta d\Omega-\int_{\mathcal{B}_t}c\rho\dot{\theta}\delta\theta d\Omega=0 \tag{2.3.11}$$

Balance of heat flux and corresponding weak forms are more elaborately discussed in Section 3.5.

2.4 Change in observer and Invariance of reference frame

Use of two coordinate systems, like the spatial and the material ones, or the co-rotational one, which moves fixed to some specific direction with the body, is one of the artistry of mechanics that eases the analysis of the system. Use of two reference coordinates, or rather two different observers generally means that there exists two different views of the body with respect to the different observers. Let us consider two motions $\tilde{x}(t)$ and $\tilde{x}^*(t)$ of a body $\mathcal{B}_t$ as shown in Figure 2.5. Then $\tilde{x}$ and $\tilde{x}^*$ is related by

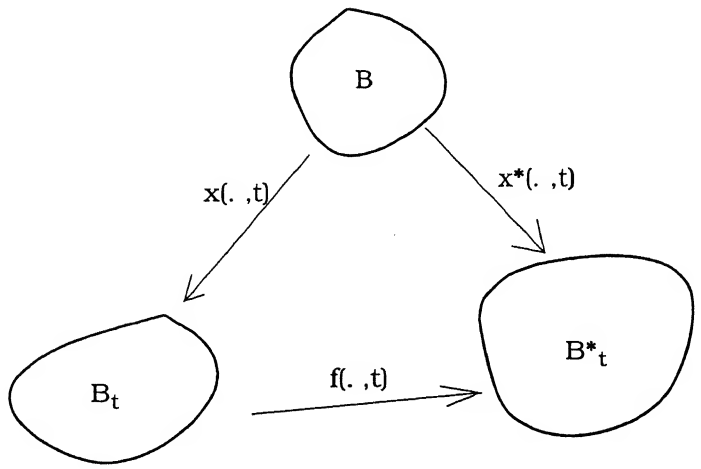

Figure 2.5: Two reference systems

the relation

$$\tilde{x}^*(\tilde{X},t) = \tilde{q}(t) + \tilde{\tilde{Q}}(t)[\tilde{x}(\tilde{X},t) - \tilde{0}] \tag{2.4.1}$$

for every material point $\tilde{X}$ and time t, where $\tilde{q}$ is a point in space and $\tilde{\tilde{Q}}$ is a rotation. This is equivalent to define a one-to-one mapping $\tilde{f}(\tilde{x},t)$ as:

$$\tilde{f}(\tilde{x},t) = \tilde{q}(t) + \tilde{\tilde{Q}}(t)(\tilde{x} - \tilde{0})$$

and representing $\tilde{x}^*$ as the deformation $\tilde{x}$ followed by a rigid deformation $\tilde{f}$[1]. That is,

$$\tilde{x}^*(.,t) = \tilde{f}(.,t) \circ \tilde{x}(.,t)$$

As shown in Figure 2.5, the two observer coordinates $\tilde{x}$ and $\tilde{x}^*$ are related as:

$$\tilde{x}^* = \tilde{f}(\tilde{x},t)$$

And the inverse mapping,

$$\tilde{x} = \tilde{f}^{-1} \circ \tilde{x}^*$$

is also true. Inverting this relation to the material coordinate frame, it turns out to be

$$\tilde{X}(.,t) = \tilde{X}^*(.,t) \circ \tilde{f}(.,t)$$

The term **objectivity** means the invariance of the various kinematic quantities under the change of reference system. The laws of mechanics should strictly follow the transformation laws between the two deformation mappings $\tilde{x}$ and $\tilde{x}^*$. The basic relations of the different quantities are derived in this section.

Let,

$$\tilde{\tilde{F}} = \frac{\partial \tilde{x}}{\partial \tilde{X}}$$

$$\text{and } \tilde{\tilde{F}}^* = \frac{\partial \tilde{x}^*}{\partial \tilde{X}}$$

differentiating Equation 2.4.1,

$$\tilde{\tilde{F}}^*(\tilde{X},t) = \tilde{\tilde{Q}}(t)\tilde{\tilde{F}}(\tilde{X},t) \tag{2.4.2}$$

[1] As both the frames $\tilde{x}$ and $\tilde{x}^*$ are mutually orthogonal triad, any one of them can be transformed to the other simply by a rigid rotation, namely $\tilde{\tilde{Q}}$

Equation 2.4.2 gives the transformation law for the deformation gradient. As the tensor $\tilde{\tilde{Q}}$ represents a rigid deformation, $det(\tilde{\tilde{Q}}) = 1$, i.e.

$$det(\tilde{\tilde{F}}) = det(\tilde{\tilde{F}}^*) \text{ [as det(ab)=det(a) det(b)]} \tag{2.4.3}$$

This confirms the fact that the volume of the deformed body $\mathcal{B}_t$ should remain same for both the observers.
Also, let the polar decomposition of the deformation gradients be

$$\tilde{\tilde{F}}^* = \tilde{\tilde{R}}^* \tilde{\tilde{U}}^* = \tilde{\tilde{V}}^* \tilde{\tilde{R}}^*$$
$$\tilde{\tilde{F}} = \tilde{\tilde{R}} \tilde{\tilde{U}} = \tilde{\tilde{V}} \tilde{\tilde{R}}$$

From Equation 2.4.2,

$$\begin{aligned} \tilde{\tilde{F}}^* = \tilde{\tilde{R}}^* \tilde{\tilde{U}}^* &= \tilde{\tilde{Q}} \tilde{\tilde{F}} \\ &= \tilde{\tilde{Q}} \tilde{\tilde{R}} \tilde{\tilde{U}} \end{aligned}$$

Since both $\tilde{\tilde{Q}}$ and $\tilde{\tilde{R}}$ are elements of the vector space formed by the rotation tensors,

$$\tilde{\tilde{R}}^* = \tilde{\tilde{Q}} \tilde{\tilde{R}} \tag{2.4.4}$$

and

$$\tilde{\tilde{U}}^* = \tilde{\tilde{U}} \tag{2.4.5}$$

i.e the stretch $\tilde{\tilde{U}}$ remains same for the two different observers. The only difference in the deformation gradient comes from the rotational parts. The corresponding rotation should be transformed as in Equation 2.4.4. From Equation 2.4.5, the right Cauchy-Green strain tensors for the two different observers also remains same

$$\tilde{\tilde{C}} = \tilde{\tilde{U}}^2$$
$$\begin{aligned} \text{and, } \tilde{\tilde{C}}^* &= \tilde{\tilde{F}}^{*T} \tilde{\tilde{F}}^* \\ &= \tilde{\tilde{U}}^{*T} \tilde{\tilde{R}}^{*T} \tilde{\tilde{R}}^* \tilde{\tilde{U}}^* \\ &= \tilde{\tilde{U}}^{*T} \tilde{\tilde{U}}^* \text{ [as } \tilde{\tilde{R}}^* \text{ is orthogonal]} \\ &= \tilde{\tilde{U}}^2 \end{aligned}$$

And the left Cauchy-Green strain tensors are related as follows:

$$\begin{aligned}\tilde{\tilde{B}}^* &= \tilde{\tilde{F}}^* \tilde{\tilde{F}}^{*T} \\ &= \tilde{\tilde{Q}} \tilde{\tilde{F}} \tilde{\tilde{F}}^T \tilde{\tilde{Q}}^T \\ &= \tilde{\tilde{Q}} \tilde{\tilde{B}} \tilde{\tilde{Q}}^T \text{ [as } \tilde{\tilde{F}} \tilde{\tilde{F}}^T = \tilde{\tilde{B}}]\end{aligned}$$

Now, referring to Figure 2.6, the axiom of change of observer states that,

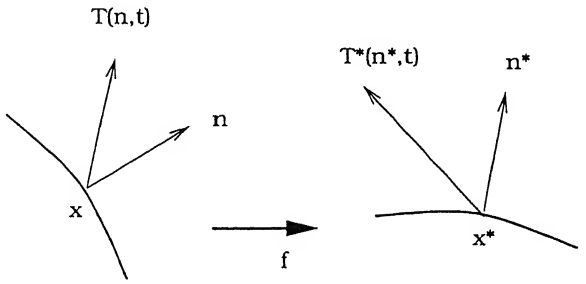

Figure 2.6: Surface force density function with respect to the two different observers

$$\tilde{n}^* = \tilde{\tilde{Q}} \tilde{n}$$

And as

$$\tilde{\tilde{Q}} = \tilde{\tilde{Q}}(t)$$

We can also write

$$\tilde{T}^*(\tilde{n}^*) = \tilde{\tilde{Q}} \tilde{T}(\tilde{n})$$

Using $\tilde{T} = \tilde{\tilde{\sigma}} \tilde{n}$ and $\tilde{T}^* = \tilde{\tilde{\sigma}}^* \tilde{n}^*$,

$$\begin{aligned}\tilde{T}^* = \tilde{\tilde{\sigma}}^* \tilde{n}^* &= \tilde{\tilde{Q}} \tilde{T} \\ &= \tilde{\tilde{Q}} \tilde{\tilde{\sigma}} \tilde{n} \\ &= \tilde{\tilde{Q}} \tilde{\tilde{\sigma}} \tilde{\tilde{Q}}^T \tilde{n}^* \text{ [as } \tilde{\tilde{Q}}^{-1} = \tilde{\tilde{Q}}^T]\end{aligned}$$

Hence,

$$\tilde{\tilde{\sigma}}^*(\tilde{x}^*, t) = \tilde{\tilde{Q}}(t) \tilde{\tilde{\sigma}}(\tilde{x}, t) \tilde{\tilde{Q}}^T(t) \tag{2.4.6}$$

Equation 2.4.6 gives the transformation rule for the stress tensor for a rigid rotation $\tilde{\tilde{Q}}$ to the observer's reference system.

2.5 Eulerian approach

As mentioned earlier, the basic idea of the Eulerian type of analysis is to study the continuum with the observer fixed at the Eulerian or spatial coordinate system. It is like studying the kinematic and kinetic characteristics of some spatially fixed (with respect to the stars) points for some interval of time. As this approach, by definition, accepts that the material points under study (at the fixed point at current time) may not, or rather, shall not be the unique one, so, it is not possible to study the motion or displacement of any material point in this scheme. Instead, the velocity and accelerations are considered to be the primary parameters of investigation at the fixed points of interest. This understanding is somewhat analogous to the control volume analysis of fluids.

2.6 Lagrangian approach

Here, the idea is that the parameters under study are the ones related to the material points. The formulation is in terms of Lagrangian measures of stress and strain, and the derivatives and integrals are defined over the material reference frame. The material coordinates are expressed as some discrete function of the spatial coordinates. This is obtained by freezing the time at the instant of observation. The instant at which the system is frozen to the observer defines the types of Lagrangian methods, namely the Updated Lagrangian or Total Lagrangian.

In **Total Lagrangian(TL)** method, the configuration of the body at time t=0 (from when the analysis starts) is taken as the reference configuration for the whole analysis. The balance laws of mechanics are transformed to the configuration at time 0 from the currently deformed, unknown configuration. Whereas in **Updated Lagrangian(UL)** approach, the reference configuration is continuously updated with time. i.e., the whole time period under analysis is divided into some small time windows and for each time window, the TL approach is carried out. For the first step, the reference configuration is the body at time 0. And for the next step onwards, the reference configuration used in a specific UL step is nothing but the deformed configuration (output from the previous step) obtained from the previous step. Both UL and TL formulations are theoretically equivalent, but the only difference for UL method is that the configuration at time t is considered as the initial configuration, where for TL, it is the configuration at time 0 [3]. Hence the UL method is nothing but the TL method by steps and is used while handling non-linear problems to get the numerics better.

2.7 UL Method and incremental form

The target in UL method, as aforementioned, is to solve for the unknown parameters over some pre-defined time steps, called UL steps, each of time size Δt (Δt may vary from step to step). For any generic time step with initial time as t, the unknown parameters are to be solved for the time $t + \Delta t$ from the known configuration at current time t. As the configuration of the body at that time, $\mathcal{B}_{t+\Delta t}$ is an unknown itself, it is not possible to solve the momentum balance equation directly for time $t + \Delta t$

(as it is basically a force balance over the unknown domain). The individual terms of the momentum balance law as well as the domain of definition of it, must be transformed to the ones at currently known time by using proper transformation laws. For small deformations, these two configurations, $\mathcal{B}_{t+\Delta t}$ and $\mathcal{B}_t$ may be considered to be the same and the the momentum balance equation or its weak form can be solved directly in a total form defined over the domain at time t. But for large deformation and large rotation systems, this may lead to a completely different solution than the exact one.
But the problem in this transformation, basically transformation of the equation of the principle of virtual work from the deformed configuration to the undeformed one, makes the resulting equation a rather complex one and with a lot more non-linear terms. And in this transformation, it is also convenient to use the **incremental form** instead of the total form. Detailed deductions are provided in Section 3.2. This is nothing but defining the primary unknowns at time $t+\Delta t$ as a linear increment over their current values as:

$$\tilde{u}_{t+\Delta t} = \tilde{u}_t + \Delta u \tag{2.7.1}$$

and

$$\tilde{\tilde{\sigma}}_{t+\Delta t} = \tilde{\tilde{\sigma}}_t + \Delta\tilde{\tilde{\sigma}} \tag{2.7.2}$$

and so on.

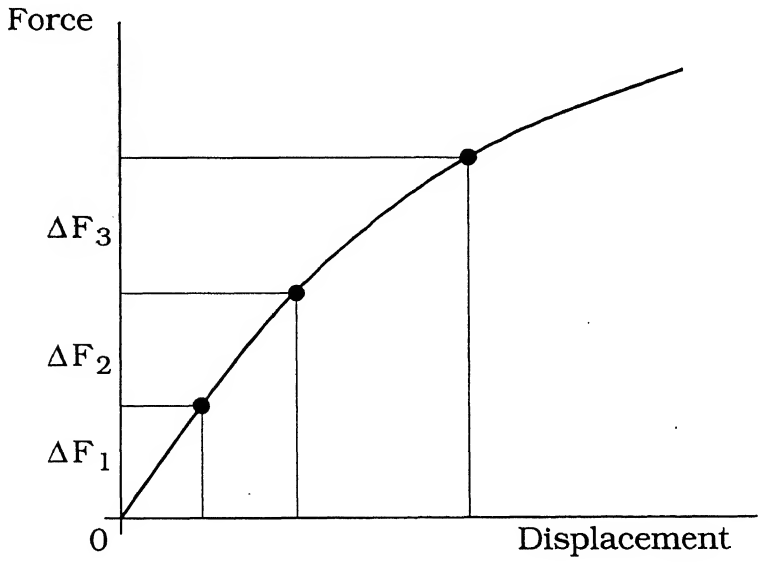

Figure 2.7: Quasi-static UL formulation

For the static analysis, the quasi-static form of the UL method is used. As there is no time parameter in the formulation for static problem, the total force $\tilde{F}_{ext}$ is divided in some incremental forces like ΔF_1, ΔF_2 and so on as shown in the Figure 2.7. The system is analyzed for each force step cumulatively for each ΔF_{ext}. The configuration obtained from the previous is the input configuration for the next step.

Chapter 3

Theoretical formulations

3.1 Balance law in deformed configuration

In the current work, the deduction of the momentum conservation equation and corresponding weak forms are done by giving proper honor to the instances of time when they are defined and hence to the related reference frames also. The governing differential equation(GDE) is the momentum balance equation defined at the deformed configuration. The conservation of momentum, defined at a specific configuration, say $\mathcal{B}_t$, is expressed as:

$$\int_{\partial\mathcal{B}_t} \tilde{T} dS + \int_{\mathcal{B}_t} \rho\tilde{b} d\Omega = \int_{\mathcal{B}_t} \rho\ddot{\tilde{u}} d\Omega \tag{3.1.1}$$

Replacing $\tilde{T}$ from Cauchy's theorem as $\tilde{T} = \tilde{\tilde{\sigma}}\tilde{n}$, and using Gauss divergence theorem, the momentum balance equation can be written in a point-wise sense as:

$$\int_{\mathcal{B}_t} [div\tilde{\tilde{\sigma}} + \rho\tilde{b}] d\Omega = \int_{\mathcal{B}_t} \rho\ddot{\tilde{u}} d\Omega \tag{3.1.2}$$

Perturbing the system by a kinematically admissible virtual displacement field $\delta\tilde{u}$ the weak form of the momentum balance becomes analogous to the theorem of virtual work (Equation 2.3.9) in the deformed configuration $\mathcal{B}_t$:

$$\int_{\mathcal{B}_t} \rho\ddot{\tilde{u}} \cdot \delta\tilde{u} d\Omega + \int_{\mathcal{B}_t} \tilde{\tilde{\sigma}} : \frac{\partial\delta\tilde{u}}{\partial\tilde{x}} d\Omega - \int_{\mathcal{B}_t} \rho\tilde{b} \cdot \delta\tilde{u} d\Omega - \int_{\partial\mathcal{B}_t} \tilde{T} \cdot \delta\tilde{u} dS = 0 \tag{3.1.3}$$

3.2 Transformation of weak form to undeformed coordinate and incremental weak form

The target of Lagrangian formulation is to bring the momentum balance equation from the unknown deformed configuration to the currently known and undeformed configuration. As shown in Figure 2.1, the momentum balance equation is defined at the configuration $\mathcal{B}_{t+\Delta t}$ which is currently unknown.

So, the target is to form the momentum conservation law, or rather it's weak form in the deformed configuration and then transfer the same to the undeformed configuration for that time step (i.e to the Lagrangian reference frame defined over time t). This transformation from $t+\Delta t$ to time t is dependent on the displacement gradient from time $t+\Delta t$ to t, which is shown as tensor $\tilde{\tilde{G}}$ in Figure 2.1.
This displacement gradient $\tilde{\tilde{G}}$, may be called the incremental displacement gradient as it is analogous to the other incremental parameters from time t to $t+\Delta t$, and can be found out in terms of unknown incremental displacements from Figure 2.1, using the definition of the corresponding parameters as follows.

$$\tilde{\tilde{F}}_t = \frac{\partial \tilde{x}_t}{\partial \tilde{X}}$$

and

$$\begin{aligned}
\tilde{\tilde{F}}_{t+\Delta t} &= \frac{\partial \tilde{x}_{t+\Delta t}}{\partial \tilde{X}} \\
&= \frac{\partial (\tilde{X} + \tilde{u}_{t+\Delta t})}{\partial \tilde{X}} \\
&= \frac{\partial (\tilde{X} + \tilde{u}_t + \Delta \tilde{u})}{\partial \tilde{X}} \\
&= \tilde{\tilde{F}}_t + \frac{\partial \Delta \tilde{u}}{\partial \tilde{X}}
\end{aligned}$$

So,

$$\tilde{\tilde{F}}_{t+\Delta t} = \left(\tilde{\tilde{I}} + \frac{\partial \Delta \tilde{u}}{\partial \tilde{x}_t} \right) \tilde{\tilde{F}}_t \tag{3.2.1}$$

And by definition of the incremental displacement gradient, it operates on the displacement gradient at time $t(\tilde{\tilde{F}}_t)$to give the displacement gradient at time $t+\Delta t(\tilde{\tilde{F}}_{t+\Delta t})$. That means,

$$\tilde{\tilde{F}}_{t+\Delta t} = \tilde{\tilde{G}} \circ \tilde{\tilde{F}}_t \tag{3.2.2}$$

Comparing Equation 3.2.1 and Equation 3.2.2, the incremental deformation gradient $\tilde{\tilde{G}}$ can be expressed as:

$$\tilde{\tilde{G}} \equiv \left(\tilde{\tilde{I}} + \frac{\partial \Delta \tilde{u}}{\partial \tilde{x}_t} \right) \tag{3.2.3}$$

To transform the weak form from the deformed to the undeformed coordinate, first of all, the weak forms at those configurations are to be found. And for that, the kinematically admissible displacement fields at both time instances t and $t+\Delta t$ should be known. But as the essential boundary conditions are also defined at time t, hence, only the admissible displacement field at time t is known.
Here, it is assumed that for both time instances, the displacement field has the same kinematic constraints. So, it is possible to use the same virtual displacement $\delta \tilde{u}$ for both the cases.
Then, the momentum equilibrium at the deformed configuration $B_{t+\Delta t}$ is just the same like Equation 3.1.3 with the integration limit changed over the domain of the body at time $t+\Delta t$ (i.e the deformed

configuration),

$$\int_{\mathcal{B}_{t+\Delta t}} \rho \ddot{\tilde{u}} \cdot \delta\tilde{u} d\Omega + \int_{\mathcal{B}_{t+\Delta t}} \tilde{\tilde{\sigma}} : \frac{\partial \delta\tilde{u}}{\partial \tilde{x}} d\Omega - \int_{\mathcal{B}_{t+\Delta t}} \rho \tilde{b} \cdot \delta\tilde{u} d\Omega - \int_{\partial\mathcal{B}_{t+\Delta t}} \tilde{T} \cdot \delta\tilde{u} d\Gamma = 0 \tag{3.2.4}$$

Transforming Equation 3.2.4 to the configuration at time t and writing it in point-wise form [1],

$$\int_{\mathcal{B}_t} det\tilde{\tilde{G}}[div\left(\tilde{\tilde{\sigma}}_{t+\Delta t}\delta\tilde{u}\right) - \tilde{\tilde{\sigma}}_{t+\Delta t} : \frac{\partial \delta\tilde{u}}{\partial \tilde{x}}]d\Omega + \int_{\mathcal{B}_t} \rho_t \tilde{b}_{t+\Delta t} \cdot \delta\tilde{u} d\Omega = \int_{\mathcal{B}_t} \rho_t \ddot{\tilde{u}}_{t+\Delta t} \cdot \delta\tilde{u} d\Omega \tag{3.2.5}$$

And the weak form of momentum balance at time t itself is,

$$\int_{\mathcal{B}_t} [div\left(\tilde{\tilde{\sigma}}_t\delta\tilde{u}\right) - \tilde{\tilde{\sigma}}_t : \frac{\partial \delta\tilde{u}}{\partial \tilde{x}}]d\Omega + \int_{\mathcal{B}_t} \rho_t \tilde{b}_t \cdot \delta\tilde{u} d\Omega = \int_{\mathcal{B}_t} \rho_t \ddot{\tilde{u}}_t \cdot \delta\tilde{u} d\Omega \tag{3.2.6}$$

Eliminating Equation 3.2.6 from Equation 3.2.5, the incremental form of the virtual work turns out to be,

$$\begin{aligned} \int_{\mathcal{B}_t} [det\tilde{\tilde{G}}\{div\left(\tilde{\tilde{\sigma}}_{t+\Delta t}\delta\tilde{u}\right) - \tilde{\tilde{\sigma}}_{t+\Delta t} : \frac{\partial \delta\tilde{u}}{\partial \tilde{x}}\} - div\left(\tilde{\tilde{\sigma}}_t\delta\tilde{u}\right) + \tilde{\tilde{\sigma}}_t : \frac{\partial \delta\tilde{u}}{\partial \tilde{x}}]d\Omega \\ + \int_{\mathcal{B}_t} \rho_t[\tilde{b}_{t+\Delta t} - \tilde{b}_t] \cdot \delta\tilde{u} d\Omega = \int_{\mathcal{B}_t} \rho_t[\ddot{\tilde{u}}_{t+\Delta t} - \ddot{\tilde{u}}_t] \cdot \delta\tilde{u} d\Omega \end{aligned} \tag{3.2.7}$$

Assuming $\tilde{u}_{t+\Delta t} = \tilde{u}_t + \Delta\tilde{u}$ and $\tilde{\tilde{\sigma}}_{t+\Delta t} = \tilde{\tilde{\sigma}}_t + \Delta\tilde{\tilde{\sigma}}$, Equation 3.2.7 can be modified to have $\Delta\tilde{u}$ as the primary unknown in it as,

$$\begin{aligned} \int_{\mathcal{B}_t} [det\tilde{\tilde{G}}\ div\left(\tilde{\tilde{\sigma}}_{t+\Delta t}\delta\tilde{u}\right) - div\left(\tilde{\tilde{\sigma}}_t\delta\tilde{u}\right)]d\Omega + \int_{\mathcal{B}_t} \rho_t \Delta\tilde{b} \cdot \delta\tilde{u} d\Omega \\ = \int_{\mathcal{B}_t} \rho_t \Delta\ddot{\tilde{u}} \cdot \delta\tilde{u} d\Omega + \int_{\mathcal{B}_t} \Delta\tilde{\tilde{\sigma}} : \frac{\partial \delta\tilde{u}}{\partial \tilde{x}} d\Omega \end{aligned} \tag{3.2.8}$$

The first term of Equation 3.2.8 can be expanded as,

$$\begin{aligned} \int_{\mathcal{B}_t} \left[det\tilde{\tilde{G}}\ div\left(\tilde{\tilde{\sigma}}_{t+\Delta t}\delta\tilde{u}\right) - div\left(\tilde{\tilde{\sigma}}_t\delta\tilde{u}\right)\right] d\Omega &= \int_{\partial\mathcal{B}_t} \left[det\tilde{\tilde{G}}\ \tilde{\tilde{\sigma}}_{t+\Delta t}\delta\tilde{u} \cdot \tilde{n}_t - \tilde{\tilde{\sigma}}_t\delta\tilde{u} \cdot \tilde{n}_t\right] dS \\ &= \int_{\partial\mathcal{B}_t} \left[det\tilde{\tilde{G}}\ \tilde{\tilde{\sigma}}_{t+\Delta t}\tilde{n}_t \cdot \delta\tilde{u} - \tilde{\tilde{\sigma}}_t\tilde{n}_t \cdot \delta\tilde{u}\right] dS \\ &= \int_{\partial\mathcal{B}_t} \left[det\tilde{\tilde{G}}\ (\tilde{\tilde{\sigma}}_t + \Delta\tilde{\tilde{\sigma}})\tilde{n}_t \cdot \delta\tilde{u} - \tilde{\tilde{\sigma}}_t\tilde{n}_t \cdot \delta\tilde{u}\right] dS \end{aligned}$$

Hence,

$$\int_{\mathcal{B}_t} \left[det\tilde{\tilde{G}}\ div\left(\tilde{\tilde{\sigma}}_{t+\Delta t}\delta\tilde{u}\right) - div\left(\tilde{\tilde{\sigma}}_t\delta\tilde{u}\right)\right] d\Omega = \int_{\partial\mathcal{B}_t} \left[det\tilde{\tilde{G}}\ (\tilde{\tilde{\sigma}}_t + \Delta\tilde{\tilde{\sigma}})\tilde{n}_t \cdot \delta\tilde{u} - \tilde{\tilde{\sigma}}_t\tilde{n}_t \cdot \delta\tilde{u}\right] dS \tag{3.2.9}$$

It is assumed that the traction forces on boundary do not change with configuration of the body, i.e there are no follower loads. Then, the effect of change of normal on the traction force term shown in

Equation 3.2.9 can be thrown out.
Thus, on applying the Gauss divergence theorem,

$$\int_{\mathcal{B}_t} \rho_t \Delta\ddot{\tilde{u}} \cdot \delta\tilde{u} d\Omega + \int_{\mathcal{B}_t} \Delta\tilde{\tilde{\sigma}} : \frac{\partial \delta\tilde{u}}{\partial \tilde{x}} d\Omega = \int_{\mathcal{B}_t} \rho_t \Delta\tilde{b} \cdot \delta\tilde{u} d\Omega + \int_{\partial\mathcal{B}_t} \Delta\tilde{T} \cdot \delta\tilde{u} dS \tag{3.2.10}$$

Equation 3.2.10 is the incremental weak form of the momentum equation in material coordinates.
The assumption that the kinematic admissible conditions on the virtual displacement field $\delta\tilde{u}$ remains same for both configurations $\mathcal{B}_t$ and $\mathcal{B}_{t+\Delta t}$, is valid as there is no change in the kinematic constraints in the two configurations.
Obviously, this assumption doesn't remain valid for large deformation contact problems. Then the constraints are very likely to be changed within the time span Δt continuously. For those kind of formulation, the virtual displacement field should also be considered as a function of the spatial coordinate and time, i.e $\delta\tilde{u} = \delta\tilde{u}(\tilde{x}, t)$.

3.3 Objective stress increment - Jaumann Zaremba stress rate for small deformation

As mentioned in Section 2.4, objectivity is an issue of importance when two types of reference frames, namely spatial and material reference frames, are considered in the analysis. The kinematics of a body appears to be different to two different observers situated in the two different reference frames. The basic idea of using the objectivite measures is nothing but just honoring the difference between the observations of the two observers. Objectivity for rigid rotation generally means a set of transformation rule to be implemented between two reference coordinates to transform some quantities defined in one coordinate to another.
Equation 2.4.1 and Equation 2.4.6 state the general rules for objective transformation of any kinematic vector and kinematic tensor respectively for the configurations shown in Figure 2.5.
For large strain and large rotation analysis, the value of the increment in Cauchy stress due to the rigid rotation of the deformed coordinate with respect to the undeformed one, is never negligible. For the incremental displacement field $\Delta\tilde{u}$, the rigid rotation part of the whole deformation from time t to $t+\Delta t$ can be found out by decomposing the corresponding incremental displacement gradient $\tilde{\tilde{G}} = (\tilde{\tilde{I}} + \frac{\partial \Delta\tilde{u}}{\partial x_t})$ by polar decomposition. Let the decomposition of the incremental displacement gradient be as,

$$\tilde{\tilde{G}} = \tilde{\tilde{R}}\tilde{\tilde{U}}$$

by the right polar decomposition.
Here, $\tilde{\tilde{R}}$ is the rigid rotation tensor and $\tilde{\tilde{U}}$ is the stretch tensor.

As $\tilde{\tilde{R}}$ is an orthogonal tensor,

$$\begin{aligned}\tilde{\tilde{U}}^2 &= \tilde{\tilde{G}}^T\tilde{\tilde{G}} \\ &= \left(\tilde{\tilde{I}} + \frac{\partial\Delta\tilde{u}}{\partial\tilde{x}_t}\right)^T\left(\tilde{\tilde{I}} + \frac{\partial\Delta\tilde{u}}{\partial\tilde{x}_t}\right) \\ &= \tilde{\tilde{I}} + \frac{\partial\Delta\tilde{u}}{\partial\tilde{x}_t} + \left(\frac{\partial\Delta\tilde{u}}{\partial\tilde{x}_t}\right)^T + \left(\frac{\partial\Delta\tilde{u}}{\partial\tilde{x}_t}\right)^T\frac{\partial\Delta\tilde{u}}{\partial\tilde{x}_t}\end{aligned}$$

Assuming the incremental deformations considered to be small and using binomial expansion [1]

$$\begin{aligned}\tilde{\tilde{U}} &= \sqrt{\tilde{\tilde{U}}^2} \\ &\simeq \sqrt{\tilde{\tilde{I}} + \frac{\partial\Delta\tilde{u}}{\partial\tilde{x}_t} + \left(\frac{\partial\Delta\tilde{u}}{\partial\tilde{x}_t}\right)^T} \\ &\simeq \tilde{\tilde{I}} + \frac{1}{2}\left(\frac{\partial\Delta\tilde{u}}{\partial\tilde{x}_t} + \frac{\partial\Delta\tilde{u}}{\partial\tilde{x}_t}^T\right) \\ &= \tilde{\tilde{I}} + \tilde{\tilde{D}}\end{aligned}$$

where $\tilde{\tilde{D}}$ is the symmetric part of the tensor $\frac{\partial\Delta\tilde{u}}{\partial\tilde{x}_t}$, and

$$\begin{aligned}\tilde{\tilde{R}} &= \tilde{\tilde{G}}\tilde{\tilde{U}}^{-1} \\ &\simeq \left(\tilde{\tilde{I}} + \frac{\partial\Delta\tilde{u}}{\partial\tilde{x}_t}\right)\left\{\tilde{\tilde{I}} - \frac{1}{2}\left(\frac{\partial\Delta\tilde{u}}{\partial\tilde{x}_t} + \frac{\partial\Delta\tilde{u}}{\partial\tilde{x}_t}^T\right)\right\} \\ &= \tilde{\tilde{I}} + \frac{1}{2}\left(\frac{\partial\Delta\tilde{u}}{\partial\tilde{x}_t} - \frac{\partial\Delta\tilde{u}}{\partial\tilde{x}_t}^T\right) \\ &= \tilde{\tilde{I}} + \tilde{\tilde{W}}\end{aligned}$$

where $\tilde{\tilde{W}}$ is the rigid rotational part of the tensor $\frac{\partial\Delta\tilde{u}}{\partial\tilde{x}_t}$.

The tensors $\tilde{\tilde{D}}$ and $\tilde{\tilde{W}}$ are understood to be some measure of linear and rotational strains respectively. Hence, it can be stated that the transformation $\tilde{\tilde{G}}$ can be equivalently decomposed in two cumulative deformation gradients namely, the stretch $\tilde{\tilde{U}}$ and rotation $\tilde{\tilde{R}}$. The increment in stress will also have two corresponding increments. The pure stretch part $\tilde{\tilde{D}}$ causes the stress increment as

$$(\Delta\tilde{\tilde{\sigma}})_{stretch} = \tilde{\tilde{\tilde{E}}}\tilde{\tilde{D}} \tag{3.3.1}$$

[1] As any vector can be considered as the Eigen vector of the isotropic tensor $\tilde{\tilde{I}}$, hence Eigen directions of $\tilde{\tilde{D}}$ and $\left(\tilde{\tilde{I}} + \tilde{\tilde{D}}\right)$, $\tilde{\tilde{D}}$ being any general tensor, are same and the second one can be expanded using Binomial theorem.

where $\tilde{\tilde{E}}$ is the corresponding material tensor, and the rigid rotation $\tilde{\tilde{R}}$ causes the stress tensor in the deformed coordinate to be

$$\begin{aligned}(\tilde{\tilde{\sigma}}_{t+\Delta t})_{rotation} &= \tilde{\tilde{R}}\tilde{\tilde{\sigma}}_t\tilde{\tilde{R}}^T \\ &= (\tilde{\tilde{I}} + \tilde{\tilde{W}})\tilde{\tilde{\sigma}}_t(\tilde{\tilde{I}} + \tilde{\tilde{W}}^T) \\ &= \tilde{\tilde{\sigma}}_t + \tilde{\tilde{W}}\tilde{\tilde{\sigma}}_t + \tilde{\tilde{\sigma}}_t\tilde{\tilde{W}}^T + \tilde{\tilde{W}}\tilde{\tilde{\sigma}}_t\tilde{\tilde{W}}^T\end{aligned}$$

The higher order term $\tilde{\tilde{W}}\tilde{\tilde{\sigma}}_t\tilde{\tilde{W}}^T$ is neglected[1] to linearize the objective stress increment $\Delta\tilde{\tilde{\sigma}}_{rotation}$ as

$$(\Delta\tilde{\tilde{\sigma}})_{rotation} = \tilde{\tilde{W}}\tilde{\tilde{\sigma}}_t + \tilde{\tilde{\sigma}}_t\tilde{\tilde{W}}^T \tag{3.3.2}$$

From Equation 3.3.1 and Equation 3.3.2 the total stress increment turns out to be

$$\Delta\tilde{\tilde{\sigma}} = \tilde{\tilde{\tilde{E}}}\tilde{\tilde{D}} + \tilde{\tilde{W}}\tilde{\tilde{\sigma}}_t + \tilde{\tilde{\sigma}}_t\tilde{\tilde{W}}^T \tag{3.3.3}$$

By definition, the stress increment rate $\dot{\tilde{\tilde{\sigma}}}$ can be written as

$$\begin{aligned}\tilde{\tilde{\sigma}}_{t+\Delta t} &= \tilde{\tilde{\sigma}}_t + \tilde{\tilde{\tilde{E}}}\tilde{\tilde{D}} + \tilde{\tilde{W}}\tilde{\tilde{\sigma}}_t + \tilde{\tilde{\sigma}}_t\tilde{\tilde{W}}^T \\ &= \tilde{\tilde{\sigma}}_t + \int_0^{\Delta t}\dot{\tilde{\tilde{\sigma}}}dt \\ \Rightarrow \dot{\tilde{\tilde{\sigma}}} &= \dot{\tilde{\tilde{E}}}\tilde{\tilde{D}} + \dot{\tilde{\tilde{W}}}\tilde{\tilde{\sigma}}_t + \tilde{\tilde{\sigma}}_t\dot{\tilde{\tilde{W}}}^T\end{aligned}$$

The **Jaumann-Zaremba stress rate** is defined as the objective increment rate of Cauchy stress and is given by:

$$\tilde{\tilde{\sigma}}^{\Delta J} = \dot{\tilde{\tilde{E}}}\tilde{\tilde{D}} = \dot{\tilde{\tilde{\sigma}}} - (\dot{\tilde{\tilde{W}}}\tilde{\tilde{\sigma}}_t + \tilde{\tilde{\sigma}}_t\dot{\tilde{\tilde{W}}}^T) \tag{3.3.4}$$

This stress rate is the objective rate of Cauchy stress that comes out of the theoretical formulations automatically when the analysis is carried out in the spatial reference frame and assumption of small deformation is considered. The most general expression for objective stress rate, the **Oldroyd stress rate** [14, 12], and its derivation is mentioned in Section 3.4. Jaumann-Zaremba stress rate is a derivative of Oldroyd stress rate that takes care of only the linear terms.

3.4 More general objective stress rate and related approximation

Refer to Figure 2.1, the incremental deformation gradient $\tilde{\tilde{G}}$ is decomposed into a rigid rotation and a stretch. Expressions for these two components are derived in Section 3.3.

[1] The discussion on such throwing out of higher order terms and keeping the quantities still objective at the same time, is given in Section 3.4

For large strain and / or large rotations, maintaining objectivity for stress increments is very much important and this enforces the transformation rules already mentioned. In Section 3.3, some higher order terms are intentionally thrown out of the formulations to linearize the equations. In objective formulations, neglecting some higher order term may invite considerably large errors unless the terms thrown out is objective itself. Before neglecting any term in this kind of calculations, one must be careful so as not to destroy objective requirements.

3.4.1 Linear expression for objective stress increment

For a rigid rotation $\tilde{\tilde{R}}$, the objective stress transformation is given by

$$\tilde{\tilde{\sigma}}^* = \tilde{\tilde{R}}\tilde{\tilde{\sigma}}\tilde{\tilde{R}}^T$$

and as shown in Section 3.3, this can be expanded as

$$\tilde{\tilde{\sigma}}^* = \tilde{\tilde{\sigma}} + \tilde{\tilde{W}}\tilde{\tilde{\sigma}} + \tilde{\tilde{\sigma}}\tilde{\tilde{W}}^T + \tilde{\tilde{W}}\tilde{\tilde{\sigma}}\tilde{\tilde{W}}^T$$

From the definition of objectivity, the second order term $\tilde{\tilde{W}}\tilde{\tilde{\sigma}}_t\tilde{\tilde{W}}^T$ is itself an objective quantity as $\tilde{\tilde{W}}$ is the orthogonal tensor which represents the rigid rotation between the two coordinate systems. So, the first order frame indifference approximation can be made by dropping the second order term, which keeps the rest objective also as $\Delta\tilde{\tilde{\sigma}} = \tilde{\tilde{W}}\tilde{\tilde{\sigma}}_t + \tilde{\tilde{\sigma}}_t\tilde{\tilde{W}}^T$. This gives exactly the Jaumann-Zaremba stress increment rate for Cauchy stress without destroying the objectivity axioms up to the first order terms.

3.4.2 Oldroyd stress rate

As shown in Section 3.3, the Jaumann-Zaremba stress rate inherits cancellation of non-linear terms. But the derivation of the most general objective stress rate is quite different. The Oldroyd rate, sometimes referred as the general objective rate [12], is rather easy to be deduced by the rate formulation. The transformation from one reference frame to the next 'star marked' reference frame with deformation gradient as $\tilde{\tilde{G}}$ is considered. Cauchy's stress is a second order tensor and transformed as

$$\tilde{\tilde{\sigma}}^* = \tilde{\tilde{F}}\tilde{\tilde{\sigma}}\tilde{\tilde{F}}^T \tag{3.4.1}$$

Differentiating both sides,

$$\dot{\tilde{\tilde{\sigma}}}^* = \dot{\tilde{\tilde{F}}}\tilde{\tilde{\sigma}}\tilde{\tilde{F}}^T + \tilde{\tilde{F}}\dot{\tilde{\tilde{\sigma}}}\tilde{\tilde{F}}^T + \tilde{\tilde{F}}\tilde{\tilde{\sigma}}\dot{\tilde{\tilde{F}}}^T$$

Using Equation 3.4.1,

$$\dot{\tilde{\tilde{\sigma}}}^* = \left(\dot{\tilde{\tilde{F}}}\tilde{\tilde{F}}^{-1}\right)\tilde{\tilde{\sigma}}^* + \tilde{\tilde{F}}\dot{\tilde{\tilde{\sigma}}}\tilde{\tilde{F}}^T + \tilde{\tilde{\sigma}}^*\left(\tilde{\tilde{F}}^{-T}\dot{\tilde{\tilde{F}}}^T\right)$$

As the velocity gradient $\tilde{\tilde{L}}$ can be expressed as $\tilde{\tilde{L}} = \dot{\tilde{\tilde{F}}}\tilde{\tilde{F}}^{-1}$[1, 11], the objective rate of $\tilde{\tilde{\sigma}}^*$ can be written as

$$\dot{\tilde{\tilde{\sigma}}}^* = \tilde{\tilde{L}}\,\tilde{\tilde{\sigma}}^* + \dot{\tilde{\tilde{\sigma}}}^*_m + \tilde{\tilde{\sigma}}^*\,\tilde{\tilde{L}}^T \tag{3.4.2}$$

Equation 3.4.2 gives the material frame invariant relation for the time derivative of Cauchy stress tensor. The Oldroyd objective stress rate is defined as

$$\dot{\tilde{\tilde{\sigma}}}_m = \dot{\tilde{\tilde{\sigma}}} - \tilde{\tilde{L}}\,\tilde{\tilde{\sigma}} - \tilde{\tilde{\sigma}}\,\tilde{\tilde{L}}^T \tag{3.4.3}$$

This objective rate is sometimes considered as the general objective stress rate [12] and the Jaumann stress rate is deduced from it considering rotation followed by stretch (or the reverse), i.e $\tilde{\tilde{L}} = \tilde{\tilde{W}}$. But the process of polar decomposition seems more general as the two motions are separated as two operators.

3.5 Heat transfer

In the current analysis, the coupling between the effects of elastic and the thermal loading is ignored. That is, the thermo-mechanical constitutive equations (Equation 3.6.13) are considered to be isentropic. This is basically ignoring the second law of thermodynamics and removing the constraints on the entropy generation. When the analysis is assumed to be isentropic, having small quasi-static incremental steps, this kind of formulation gives a simpler system to solve.
The material under analysis is assumed to obey **Fourier's law** of heat conduction. Then the heat flux in the body in the i^{th} direction is given by [3]

$$q_i = -\,k_{ij}\theta_{,j}\ (i,j = 1\ to\ 3)$$

For a three-dimensional body, the general form of the balance of heat flux is [13]

$$(k_{xx}\theta_{,x} + k_{xy}\theta_{,y} + k_{xz}\theta_{,z})_{,x} + (k_{yx}\theta_{,x} + k_{yy}\theta_{,y} + k_{yz}\theta_{,z})_{,y} + (k_{zx}\theta_{,x} + k_{zy}\theta_{,y} + k_{zz}\theta_{,z})_{,z} + q^b - c\rho\frac{d\theta}{dt} = 0 \tag{3.5.1}$$

As the medium is considered to be isotropic and homogeneous, $k_{ij,i\neq j} = 0$ and Equation 3.5.1 becomes

$$(k_x\theta_{,x})_{,x} + (k_y\theta_{,y})_{,y} + (k_z\theta_{,z})_{,z} + q^b - c\rho\dot{\theta} = 0 \tag{3.5.2}$$

Multiplying Equation 3.5.2 by a thermally admissible virtual temperature field $\delta\theta$ and integrating over the domain of the body,

$$\int_{\mathcal{B}_{t+\Delta t}} (k_i\theta_{t+\Delta t,i})_{,i}\delta\theta d\Omega + \int_{\mathcal{B}_{t+\Delta t}} q^b_{t+\Delta t}\delta\theta d\Omega - \int_{\mathcal{B}_{t+\Delta t}} c\rho_{t+\Delta t}\dot{\theta}_{t+\Delta t}\delta\theta d\Omega = 0$$

$$or, \int_{\mathcal{B}_{t+\Delta t}} (k_i\theta_{t+\Delta t,i}\delta\theta)_{,i}d\Omega - \int_{\mathcal{B}_{t+\Delta t}} (k_i\theta_{t+\Delta t,i})\delta\theta_{,i}d\Omega + \int_{\mathcal{B}_{t+\Delta t}} q^b_{t+\Delta t}\delta\theta d\Omega - \int_{\mathcal{B}_{t+\Delta t}} c\rho_{t+\Delta t}\dot{\theta}_{t+\Delta t}\delta\theta d\Omega = 0$$

Using Gauss divergence theorem, the weak form at deformed configuration becomes

$$\int_{\partial\mathcal{B}_{t+\Delta t}} (k_i\theta_{t+\Delta t,i}\delta\theta)n_i dS - \int_{\mathcal{B}_{t+\Delta t}} (k_i\theta_{t+\Delta t,i})\delta\theta_{,i}d\Omega + \int_{\mathcal{B}_{t+\Delta t}} q^b_{t+\Delta t}\delta\theta d\Omega - \int_{\mathcal{B}_{t+\Delta t}} c\rho_{t+\Delta t}\dot{\theta}_{t+\Delta t}\delta\theta d\Omega = 0 \tag{3.5.3}$$

Weak form of Heat flow equation in the previous configuration is

$$\int_{\partial\mathcal{B}_t} (k_i\dot{\theta}_{t,i}\delta\theta)n_i dS - \int_{\mathcal{B}_t} (k_i\theta_{t,i})\delta\theta_{,i}d\Omega + \int_{\mathcal{B}_t} q^b_t\delta\theta d\Omega - \int_{\mathcal{B}_t} c\rho_t\dot{\theta}_t\delta\theta d\Omega = 0 \tag{3.5.4}$$

As in Section 3.2, the increment in temperature is also considered a linear one as $\theta_{t+\Delta t} = \theta_t + \Delta\theta$. Eliminating Equation 3.5.4 from Equation 3.5.3, assuming the higher order terms from direction change of surface normal (as shown in Section 3.2) to be negligible small and ignoring the coupling with elastic deformation, the incremental weak form for heat conduction is

$$\int_{\mathcal{B}_t} c\rho_t\Delta\dot{\theta}\delta\theta d\Omega + \int_{\mathcal{B}_t} (k_i\Delta\theta_{,i})\delta\theta_{,i}d\Omega = \int_{\mathcal{B}_t} \Delta q^b\delta\theta d\Omega + \int_{\partial\mathcal{B}_t} \Delta q^s_i n_i\delta\theta dS \tag{3.5.5}$$

where q^s_i is the surface heat flux in the i^{th} direction.

3.6 Constitutive law and corresponding assumptions

The axioms of nature of forces, or rather the laws they should follow, are defined by the momentum conservation equations. These do not define the deformation completely. Because, the relation between the amount of force and the corresponding amount of deformation is still unknown. To relate the deformation and it's type to the force field, one has to apply required constitutive assumptions to the body. In mechanics, there are mainly 3 types of constitutive assumptions used [1], namely,

(i) *Constraints on the possible deformation field of the body.* This assumption defines the type of deformation that would take place for the force. Example of this kind of constraint is like allowing the rigid motions of the body or imposing an constraint on the volume of the body like isochoric deformation.

(ii) *Assumption in the form of the stress tensor.* This kind of assumptions defines the properties of the stress tensor, e.g. symmetry for no body moments, diagonal in case of pressure load etc.

(iii) *Constitutive assumptions relating stress to deformation.* These are the conventionally used consti-

tutive equations like Hooke's law. They express the measures of force as a function of the motion. The constitutive assumptions are basically the statements of relation between the displacement field and force fields, consistent with the kinematic process $\mathcal{C}$ ($\mathcal{C}$ is called the constitutive class of the body[1]) which enforces the compatibility conditions.

3.6.1 Theories of constitutive equations

The constitutive relations must obey some laws evolved from the fundamental postulates of mechanics. Most important of those are [2, 11]
(i) principle of equipresence and
(ii) material frame indifference.

Principle of equipresence

Though this axiom has not been universally accepted, but this has a very clear physical sense and is followed by many of the analysts. This principle was first presented by Truesdell and Toupin (1960) as:

An independent variable assumed to be present in one constitutive equation of a material should be assumed to be present in all constitutive equations of the same material, unless its presence contradicts the principle of material frame-indifference or some other fundamental principle [2].

Material frame indifference

This assumption states that every constitutive equation should be objective, or independent of the rotation of the material frame they are defined at (frame indifference included in Section 2.4). This is one of the fundamental postulates of a purely mechanical body.

3.6.2 Isotropic linear elasticity

The assumption of traditional elasticity is that the stress-strain relation is not dependent on any other parameters. In other words, the general measure of tension can be represented as a function of only the general deformation [14, 11]. i.e.

$$\tilde{\tilde{\tau}} = \tilde{\tilde{\tau}}(\tilde{\tilde{\varepsilon}})$$

where $\tilde{\tilde{\tau}}$ is the general tension parameter and $\tilde{\tilde{\varepsilon}}$ is the any general deformation.
And also, in general, the word elasticity is analogous to **hyper-elasticity**. This constitutive class includes materials which have a strain energy function defined due to Green as[14]

$$\mathbb{W} = \mathbb{W}(\tilde{\tilde{\varepsilon}})$$

These materials are also called **Green-elastic**. Elasticity without any underlying strain energy function is referred as **hypoelasticity** or **Cauchy-elasticity**.
Now, for small deviation in the deformation parameter, the constitutive relations may be linearized and

the strain-energy function $\mathbb{W}$ may be expanded about an equilibrium value $\mathbb{W}_0$ by Taylor's series as

$$\mathbb{W}(\tilde{\tilde{\varepsilon}}) = \mathbb{W}_0 + \frac{\partial \mathbb{W}}{\partial \tilde{\tilde{\varepsilon}}}\Big|_0 \tilde{\tilde{\varepsilon}} + \text{ higher order terms} \tag{3.6.1}$$

Considering $\tilde{\tilde{\tau}}$ to be the work conjugate of $\tilde{\tilde{\varepsilon}}$, the work done about the equilibrium state is

$$\mathbb{W}(\tilde{\tilde{\varepsilon}}) = \mathbb{W}_0 + \tilde{\tilde{\tau}}\Big|_0 \tilde{\tilde{\varepsilon}} \tag{3.6.2}$$

Comparing Equation 3.6.1 and Equation 3.6.2,

$$\tilde{\tilde{\tau}}\Big|_0 \tilde{\tilde{\varepsilon}} = \frac{\partial \mathbb{W}}{\partial \tilde{\tilde{\varepsilon}}}\Big|_0 \tilde{\tilde{\varepsilon}}$$
$$\text{or, } (\tilde{\tilde{\tau}} - \frac{\partial \mathbb{W}}{\partial \tilde{\tilde{\varepsilon}}})\Big|_0 \tilde{\tilde{\varepsilon}} = 0$$

Hence,

$$\tilde{\tilde{\tau}} = \frac{\partial \mathbb{W}}{\partial \tilde{\tilde{\varepsilon}}} \; at \; time \; t = 0 \tag{3.6.3}$$

Now, **Generalized Hooke's law** states that each stress component depends on all of the strain components and vice-versa[14]. i.e

$$\tau_{ij} = \mathrm{C}_{ijkl}\varepsilon_{kl} \tag{3.6.4}$$

where C_{ijkl} is called the elastic constant.
From Equation 3.6.3 and Equation 3.6.4,

$$\frac{\partial \mathbb{W}}{\partial \varepsilon_{ij}} = \mathrm{C}_{ijkl}\varepsilon_{kl}$$

Or,

$$\mathrm{C}_{ijkl} = \frac{\partial^2 \mathbb{W}}{\partial \varepsilon_{ij}\partial \varepsilon_{kl}} \tag{3.6.5}$$

The constant C_{ijkl} is a 4th order tensor and is called the material tensor. There are 81 entries on that tensor, but from the symmetry

$$\frac{\partial^2 \mathbb{W}}{\partial \varepsilon_{ij}\partial \varepsilon_{kl}} = \frac{\partial^2 \mathbb{W}}{\partial \varepsilon_{kl}\partial \varepsilon_{ij}}$$

C_{ijkl} is symmetric, and only 36 terms are significant.
There is also another additional symmetry for C_{ijkl} which can be shown by changing the indices as

$$\frac{\partial^2 \mathbb{W}}{\partial \varepsilon_{ij}\partial \varepsilon_{kl}} = \frac{\partial^2 \mathbb{W}}{\partial \varepsilon_{ji}\partial \varepsilon_{kl}}$$

if the strain measure ε is symmetric[1] Thus the number of significant constitutive constants become 21. For isotropic materials, for directional symmetry, this number further reduces to 9.
For the Cauchy stress and its work conjugate Almansi strain, the linear elastic constitutive equation is

$$\sigma_{ij} = \mathrm{C}_{ijkl}\epsilon_{kl} \tag{3.6.6}$$

C_{ij}, the isentropic tensor of rank 4 can be expressed as [14]

$$\mathrm{C}_{ijkl} = \lambda\delta_{ij}\delta_{kl} + \mu\delta_{ik}\delta_{jl} + \nu\delta_{il}\delta_{jk}$$

Using the symmetry of C_{ijkl} and using Lame's constants,

$$\sigma_{ij} = \lambda\delta_{ij}\epsilon_{kk} + 2\nu\epsilon_{ij} \tag{3.6.7}$$

Using engineering constants, namely Young's modulus E and Poisson's ratio ν, the relation of Equation 3.6.7 becomes[14]

$$\sigma_{ij} = \frac{E}{(1-\nu^2)}[(1-\nu)\epsilon_{ij} + \nu\epsilon_{kk}\delta_{ij}] \tag{3.6.8}$$

For three-dimensional bodies, if the six independent entities of the Cauchy stress σ_{ij} and Almansi strain ϵ_{ij} is written in the vector form following the **Voigt notation** [4] as σ_k and ϵ_k, then the material tensor becomes a two-dimensional tensor, which operates on $\tilde{\epsilon}$ to give $\tilde{\sigma}$.
As shown in [3], the material tensor then takes a form as [3]

$$[\mathrm{C}] = \frac{E(1-\nu)}{(1+\nu)(1-2\nu)}\begin{bmatrix} 1 & \frac{\nu}{(1-\nu)} & \frac{\nu}{(1-\nu)} & 0 & 0 & 0 \\ \frac{\nu}{(1-\nu)} & 1 & \frac{\nu}{(1-\nu)} & 0 & 0 & 0 \\ \frac{\nu}{(1-\nu)} & \frac{\nu}{(1-\nu)} & 1 & 0 & 0 & 0 \\ 0 & 0 & 0 & \frac{1-2\nu}{2(1-\nu)} & 0 & 0 \\ 0 & 0 & 0 & 0 & \frac{1-2\nu}{2(1-\nu)} & 0 \\ 0 & 0 & 0 & 0 & 0 & \frac{1-2\nu}{2(1-\nu)} \end{bmatrix} \tag{3.6.9}$$

3.6.3 Thermoelastic constitutive relations

For thermodynamic constitutive law, τ and ε are the thermodynamic tension and the thermodynamic deformations respectively.
The different potentials used for thermodynamics are defined as [11]

The internal energy $\mathcal{U}$ is a potential for thermodynamic tension τ for isentropic process and Helmholtz free energy Ψ is the potential for isothermal process.
The relations among the potentials and the independent variable can be deduced from the thermo-

[1] $\varepsilon_{ij} = \varepsilon_{ji}$, hence $\frac{\partial \mathrm{W}}{\partial \varepsilon_{ij}} = \frac{\partial \mathrm{W}}{\partial \varepsilon_{ji}}$

Thermodynamic potentials	Relation	Independent variables
Internal Energy ($\mathcal{U}$)	$\mathcal{U}$	s, ε_{ij}
Helmholtz Free Energy (Ψ)	$\Psi = \mathcal{U} - s\theta$	θ, ε_{ij}
Enthalpy (h)	$h = \mathcal{U} - \tau_{ij}\varepsilon_{ij}$	s, ε_{ij}
Gibbs Function/Free Enthalpy (g)	$g = \mathcal{U} - s\theta - \tau_{ij}\varepsilon_{ij} = h - s\theta$	θ, τ_{ij}

Table 3.1: Thermodynamics potentials

mechanics as [11]

$$\begin{aligned} \tau_{ij} &= \left(\frac{\partial \Psi}{\partial \varepsilon_{ij}}\right)\Big|_{\theta} \\ \varepsilon_{ij} &= -\left(\frac{\partial h}{\partial \tau_{ij}}\right)\Big|_{s} \end{aligned} \tag{3.6.10}$$

Using Cauchy stress σ_{ij} in place of τ_{ij} and Almansi strain ϵ_{ij} in place of ε_{ij}, and expanding Helmholtz free energy by Taylor series about an equilibrium configuration 0[14],

$$\Psi(\theta, \epsilon_{ij}) = \Psi_0 + \frac{\partial \Psi}{\partial \theta}\Big|_0 (\theta - \theta_0) + \frac{\partial \Psi}{\partial \epsilon_{ij}}\Big|_0 (\epsilon_{ij} - \epsilon_{0\,ij}) + \textit{higher order terms} \tag{3.6.11}$$

The relation between for the thermodynamic potential Ψ can also be shown to be analogous to that of Equation 3.6.5

$$\mathbf{C}_{ijkl} = \rho \frac{\partial^2 \Psi}{\partial \epsilon_{ij} \partial \epsilon_{kl}} \tag{3.6.12}$$

Assumed the constant values

$$\begin{aligned} \frac{\partial^2 \Psi}{\partial \theta^2}\Big|_0 &= -\frac{1}{\theta_0}\alpha_0 \\ \frac{\partial^2 \Psi}{\partial \theta \partial \epsilon_{ij}}\Big|_0 &= -\frac{1}{\rho}\beta_{ij}^0 \\ \rho \frac{\partial^2 \Psi}{\partial \epsilon_{ij} \partial \epsilon_{kl}}\Big|_0 &= \frac{\partial \sigma_{ij}}{\partial \epsilon_{kl}}\Big|_0 = \mathbf{C}_{ijkl}^0 \end{aligned}$$

Now, from Equation 3.6.10 and Equation 3.6.11, the constitutive relations for linear thermo-elasticity can be shown as follows

$$\begin{aligned} s &= s_0 + \frac{1}{\theta_0}\alpha_0(\theta - \theta_0) + \frac{1}{\rho}\beta_{ij}^0 \epsilon_{ij} \\ \sigma_{ij} &= \sigma_{ij}^0 - \beta_{ij}^0(\theta - \theta_0) + \mathbf{C}_{ijkl}^0 \epsilon_{kl} \end{aligned} \tag{3.6.13}$$

For isentropic process, $s = s_0$, hence Equation 3.6.13 reduces to

$$\begin{aligned} \theta &= \theta_0 - \frac{\theta_0}{\rho\alpha_0}\beta^0_{ij}\epsilon_{ij} \\ \sigma_{ij} &= \sigma^0_{ij} + [\mathrm{C}^0_{ijkl} + \frac{\theta_0}{\rho\alpha_0}\beta^0_{ij}\beta^0_{kl}]\epsilon_{ij} \end{aligned} \tag{3.6.14}$$

Using the engineering constants and the coefficient of thermal expansion α, the stress-strain relation stain becomes [14]

$$\epsilon_{ij} = \frac{1}{E}[(1+\nu)\sigma_{ij} - \nu\sigma_{kk}\delta_{ij}] + \alpha(\theta - \theta_0)\delta_{ij} \tag{3.6.15}$$

Inverting Equation 3.6.15, the stress σ_{ij} can be expressed as

$$\sigma_{ij} = \mathrm{C}_{ijkl}\epsilon_{kl} - \frac{E}{(1-2\nu)}\alpha\Delta\theta\delta_{ij} \tag{3.6.16}$$

where C is the linear elastic constitutive coefficients and $\Delta\theta = (\theta - \theta_0)$. i.e, in Voigt matrix notation,

$$\begin{aligned} \{\sigma\} = \frac{E(1-\nu)}{(1+\nu)(1-2\nu)} &\begin{bmatrix} 1 & \frac{\nu}{(1-\nu)} & \frac{\nu}{(1-\nu)} & 0 & 0 & 0 \\ \frac{\nu}{(1-\nu)} & 1 & \frac{\nu}{(1-\nu)} & 0 & 0 & 0 \\ \frac{\nu}{(1-\nu)} & \frac{\nu}{(1-\nu)} & 1 & 0 & 0 & 0 \\ 0 & 0 & 0 & \frac{1-2\nu}{2(1-\nu)} & 0 & 0 \\ 0 & 0 & 0 & 0 & \frac{1-2\nu}{2(1-\nu)} & 0 \\ 0 & 0 & 0 & 0 & 0 & \frac{1-2\nu}{2(1-\nu)} \end{bmatrix}\{\epsilon\} \\ &- \frac{E}{(1-2\nu)}\begin{bmatrix} 1 & 0 & 0 & 0 & 0 & 0 \\ 0 & 1 & 0 & 0 & 0 & 0 \\ 0 & 0 & 1 & 0 & 0 & 0 \\ 0 & 0 & 0 & 0 & 0 & 0 \\ 0 & 0 & 0 & 0 & 0 & 0 \\ 0 & 0 & 0 & 0 & 0 & 0 \end{bmatrix}\alpha\Delta\theta \end{aligned} \tag{3.6.17}$$

Chapter 4

Analysis of contact constraints

The contact problem is a very complex one among all the mechanical analyses presently. As computers are used to solve the huge systems of equations, study of contact has become more solvable and interesting. In this analysis, a two body contact is formulated. The **hitting or slave** body is assumed to hit a **target or master** body (Figure 4.1) [15]. The general formulation for two deformable body systems is done in this chapter, though for the computational part, only contact with a rigid target body was considered. The main problem in analysis of large deformation contact analysis is that the assumption

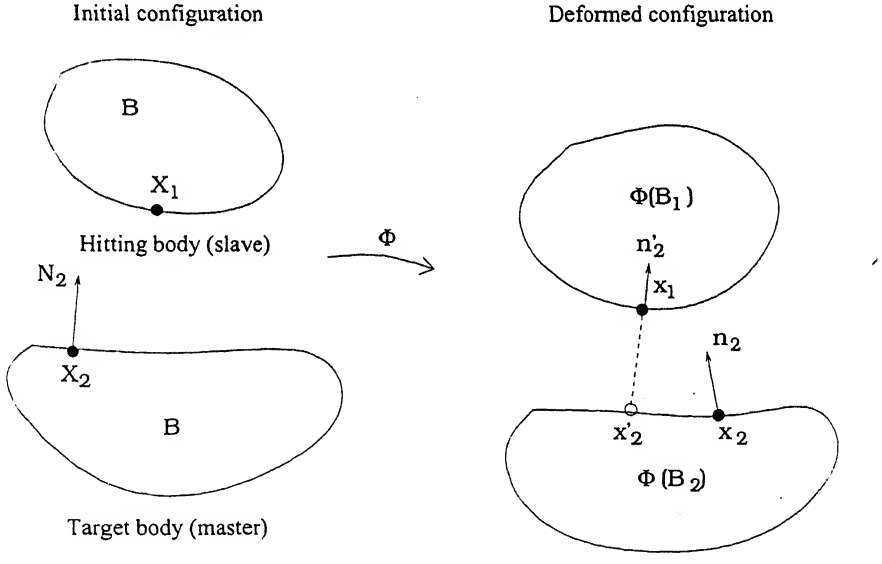

Figure 4.1: Initial and deformed configuration of contacting bodies - minimum distance

made in Section 3.2 that the kinematically admissible displacement field $\delta\tilde{u}$ remains same for both the configurations $\mathcal{B}_t$ and $\mathcal{B}_{t+\Delta t}$ does not stand valid. $\delta\tilde{u}$ should be considered as a function of time t and the spatial coordinate $\tilde{x}$ also.

But as far as small deformation contact problems are concerned, this assumption can be followed without a large amount of error caused to the results if the time steps are taken judiciously. i.e the time steps should be discretized in such a way that at the start of a particular time step, the bodies should be in

contact with each other.

4.1 Normal contact of three-dimensional bodies

In Figure 4.1, two deformable bodies are shown at their initial and deformed configuration. The contact analysis between two material points $\tilde{X}_1$ and $\tilde{X}_2$, poses a minimum distance problem to be solved in the deformed configuration as [15]

$$\|\tilde{x}_1 - \tilde{x}_2'\| = \min_{\tilde{x}_2 \subseteq \Gamma_2} \|\tilde{x}_1 - \tilde{x}_2\| \tag{4.1.1}$$

Having the point $\tilde{x}_2'$ defined on the boundary Γ_2 from Equation 4.1.1, or in other words, dropping the normal on the master surface from the slave point (considering the master surface to be at least a locally convex region, as shown in Figure 4.2), the non-penetration condition for normal contact can be stated as

$$(\tilde{x}_1 - \tilde{x}_2') \cdot \tilde{n}_2' \geq 0 \tag{4.1.2}$$

For analysis of the contact problem, Equation 4.1.2 must be imposed on the standard weak form of the problem.

4.2 Lagrangian multiplier method - penetration function

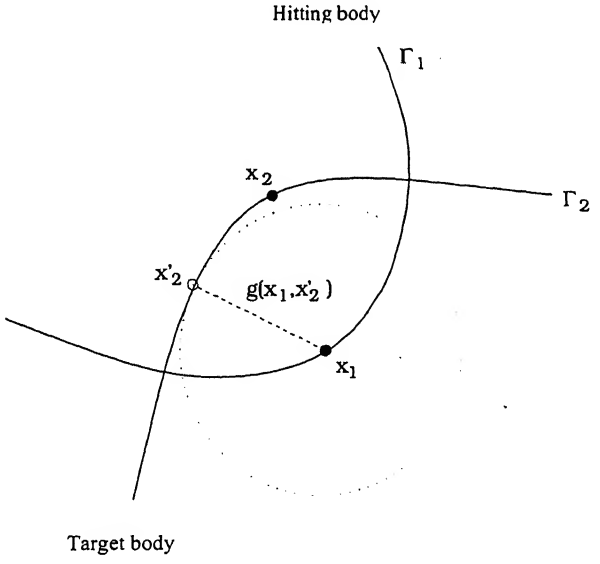

Figure 4.2: Initial and deformed configuration of contacting bodies - minimum distance

Lagrangian multiplier method is the best way to get the actual solution from the constrained (Equation 4.1.2) boundary value problem. For this approach, the non-penetration condition is modified in a

penetration function as shown in Figure 4.2 [15]

$$\tilde{g}(\tilde{x}_1, \tilde{x}_2') = \begin{cases} (\tilde{x}_1 - \tilde{x}_2') & if\ (\tilde{x}_1 - \tilde{x}_2') < 0 \\ 0 & otherwise \end{cases} \tag{4.2.1}$$

This functions is basically the gap between the two nearest points after contact [15]. The are multiplied with the unknown Lagrangian multipliers and added to the potential energy of the system, when the corresponding Lagrangian multipliers $\tilde{\lambda}$ as the corresponding contact forces at those nodes.

4.2.1 Sticking contact

For this case, the work done by the contact forces are given by

$$\Pi_{cont} = \int_{\Gamma_{cont}} \tilde{\lambda} \cdot \tilde{g} dS \tag{4.2.2}$$

The contact work from Equation 4.2.2 is added to the kinemetic potential to get the total potential energy as

$$\Pi_{total} = \Pi_{kin} + \Pi_{cont}$$
$$or,\ \delta\Pi_{total} = \delta\Pi_{kin} + \delta\Pi_{cont} = 0$$

This gives the weak form for the contact problem as

$$\int_{\mathcal{B}} \rho \ddot{\tilde{u}} \cdot \delta\tilde{u} d\Omega + \int_{\mathcal{B}} \tilde{\tilde{\sigma}} : \frac{\partial \delta\tilde{u}}{\partial \tilde{x}} d\Omega - \int_{\mathcal{B}} \rho \tilde{b} \cdot \delta\tilde{u} d\Omega - \int_{\partial\mathcal{B}} \tilde{T} \cdot \delta\tilde{u} dS - \int_{\mathcal{B}} (\tilde{\lambda} \cdot \delta\tilde{g} + \tilde{g} \cdot \delta\tilde{\lambda}) d\Omega = 0 \tag{4.2.3}$$

Again, using the assumption of small deformation that the kinematic constraints for admissible $\tilde{g}$ and $\tilde{\lambda}$ remain the same for both the configurations $\mathcal{B}_t$ and $\mathcal{B}_{t+\Delta t}$ (i.e considering virtual increment in $\tilde{g}$ and $\tilde{\lambda}$ in time t and $t + \Delta t$ to be same as in Section 3.2), the weak form of momentum equation at time $t + \Delta t$ can be written as

$$\int_{\mathcal{B}_{t+\Delta t}} \rho_{t+\Delta t} \ddot{\tilde{u}}_{t+\Delta t} \cdot \delta\tilde{u} d\Omega + \int_{\mathcal{B}_{t+\Delta t}} \tilde{\tilde{\sigma}}_{t+\Delta t} : \frac{\partial \delta\tilde{u}}{\partial \tilde{x}} d\Omega - \int_{\mathcal{B}_{t+\Delta t}} \rho_{t+\Delta t} \tilde{b}_{t+\Delta t} \cdot \delta\tilde{u} d\Omega - \int_{\partial\mathcal{B}_{t+\Delta t}} \tilde{T}_{t+\Delta t} \cdot \delta\tilde{u} dS$$
$$- \int_{\mathcal{B}_{t+\Delta t}} (\tilde{\lambda}_{t+\Delta t} \cdot \delta\tilde{g} + \tilde{g}_{t+\Delta t} \cdot \delta\tilde{\lambda}) d\Omega = 0 \tag{4.2.4}$$

Transforming Equation 4.2.4 to the undeformed configuration at time t and eliminating the weak form at time t itself from it as done in Section 3.2, the incremental weak form, after neglecting the higher

order terms, is

$$\int_{\mathcal{B}_t} \rho_t \Delta\ddot{\tilde{u}} \cdot \delta\tilde{u} d\Omega + \int_{\mathcal{B}_t} \Delta\tilde{\tilde{\sigma}} : \frac{\partial \delta\tilde{u}}{\partial \tilde{x}} d\Omega - \int_{\mathcal{B}_t} \rho_t \Delta\tilde{b} \cdot \delta\tilde{u} d\Omega - \int_{\partial\mathcal{B}_t} \Delta\tilde{T} \cdot \delta\tilde{u} dS - \int_{\mathcal{B}_t} (\Delta\tilde{\lambda} \cdot \delta\tilde{g} + \Delta\tilde{g}.\delta\tilde{\lambda}) d\Omega = 0 \tag{4.2.5}$$

4.2.2 Slipping contact with friction

The formulation is same as the sticking one, only the contact potential energy can be expressed as follows instead of Equation 4.2.2 (as the constitutive assumptions in normal and tangential directions are different)

$$\Pi_{cont} = \int_{\Gamma_{cont}} (\lambda_N g_N + \tilde{\lambda}_T \cdot \tilde{g}_T) dS \tag{4.2.6}$$

where the subscripts N and T means the normal and the tangential components respectively.
For frictional contact, Equation 4.2.6 is the constraint condition along with the corresponding frictional laws. If Coulomb's linear friction law is used, the additional constraint is given by the constitutive assumption

$$\sqrt{\lambda_{T_1}^2 + \lambda_{T_2}^2} = \mu|\lambda_N| \tag{4.2.7}$$

where λ_{T_1} and λ_{T_2} are the two components of $\tilde{\lambda}_T$.
Now, let the tangent and normal at the point $\tilde{x}_2'$ on the contact surface Γ_{cont} be as shown in Figure 4.3. The direction of the tangent is not unique, it can be taken along any convenient direction orthogonal to

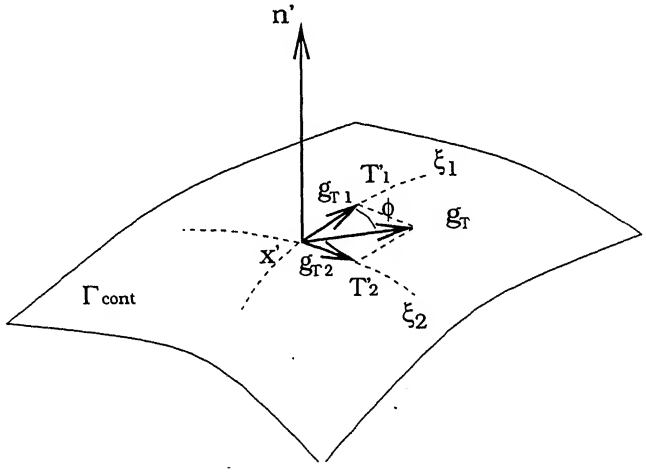

Figure 4.3: Normal and tangent at the point of contact

the direction of the normal. ξ_1 and ξ_2 are the curvilinear coordinate system at point $\tilde{x}_2'$ on surface Γ_2. Suffixes T_1 and T_2 represents the components along tangent direction T_1 and T_2.

Let ϕ be the angle between $\tilde{g}$ and $\tilde{g}_{T_1}$. Then, from Coulomb's friction laws,

$$\begin{aligned} \lambda_{T_1} &= \mu\lambda_N \cos\phi \\ \lambda_{T_2} &= \mu\lambda_N \sin\phi \\ \Rightarrow \phi &= tan^{-1}(\frac{\lambda_{T_2}}{\lambda_{T_1}}) \\ and,\ |\lambda_N| &= \frac{1}{\mu}\lambda_{T_1} \sec\phi \end{aligned} \tag{4.2.8}$$

And for discretization, it is also important to know the direction of the frictional force applied at the point of contact, By Coulomb's friction law, it is in the reverse direction of the relative slip.
Direction of relative slip between the elements at the contact is $\Delta\tilde{u}_T$ and can be related to $\Delta\tilde{u}$ as

$$\begin{aligned} \Delta\tilde{u}_T &= \Delta\tilde{u}_{T_1} + \Delta\tilde{u}_{T_2} \\ &= (\Delta\tilde{u}\cdot\tilde{T}_1)\tilde{T}_1 + (\Delta\tilde{u}\cdot\tilde{T}_2)\tilde{T}_2 \\ &= (\tilde{T}_1\otimes\tilde{T}_1)\Delta\tilde{u} + (\tilde{T}_2\tilde{\otimes}T_2)\Delta\tilde{u} \\ &= (\tilde{T}_1\otimes\tilde{T}_1 + \tilde{T}_2\otimes\tilde{T}_2)\Delta\tilde{u} \\ &= \tilde{\tilde{T}}'\Delta\tilde{u} \end{aligned} \tag{4.2.9}$$

Equation 4.2.6, 4.2.7, 4.2.8 and 4.2.9 together gives the constraint conditions applied at the contact point for the frictional slip problem [15].
Then the rest of the formulation follows the same way as the no-slip one.

Chapter 5

A brief study on continuation techniques

Continuation techniques, as the name suggests, are aimed at tracing the complete path of the load displacement curve for a structure even after a point of singularity comes in the system. In general, when a limit point is reached, i.e the slope of the load-displacement curve becomes perfectly horizontal or vertical, several problems in solution procedure appears.
As an example, in Figure 5.1(a), a load-displacement curve is shown. For simple UL solution algorithm used, a load step increment is used, and once the solution has reached point A on the curve, after the next load increment, however small it may be, it will jump to point C, instead of going to point B to capture the curve perfectly. To resolve this problem, a **displacement control method** can be used.

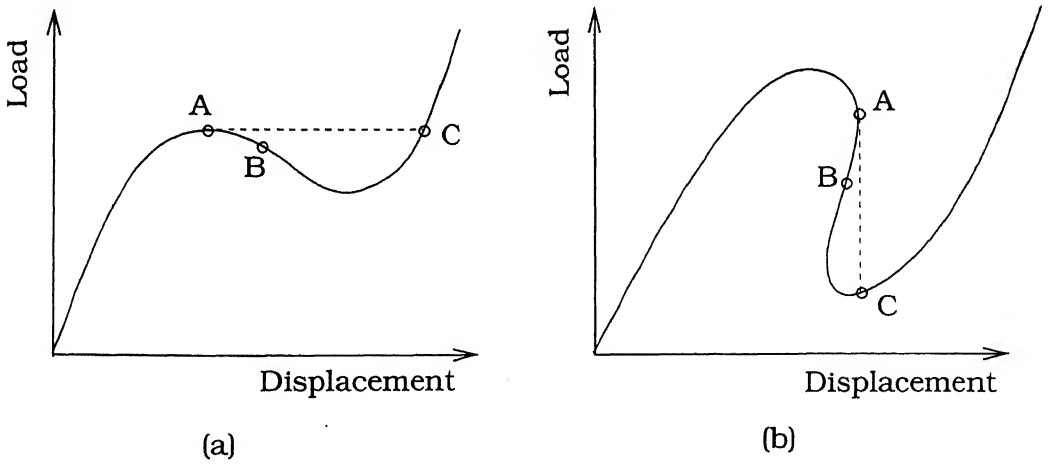

Figure 5.1: Various load - displacement curves: (a) Snap-through, (b) Snap-back

The most simple displacement control is just incrementing the displacement field by some admissible amount and calculating the corresponding force to balance the system. [1]

[1] This process has a problem for multiple variable problems. It is next to impossible to foretell the admissible displacement fi eld the structure is going to pass through in the next time step. Assigning some specifi ed fi elds may ruin the solution path completely and take the converged result to somewhere else than the actual one.
But for single variable problem, this works fi ne as any assumed displacement is an admissible one.

But this method also fails for the case shown in Figure 5.1(b), i.e a snap-back behavior of the structure. Then also, the solution simply jumps from point A to C ignoring the actual curve going through point B.
The best solution to this problem is a **mixed control** technique. i.e both the displacement and the force fields are incremented in a very controlled and defined way to track the actual path of the load-displacement curve. The most elementary type of this technique is the **Arc-length control method**.

5.1 Generalized load-displacement control

This section is targeted to cover the elementary idea of various continuation methods. In general load-displacement control, the target is to trace the actual path of the load-displacement curve by judiciously controlling both the load and the displacement fields. This is done by considering displacement as well as load, as variable quantities in the momentum balance equation used. To solve for the extra unknowns, some specific relation between the displacement and the force field is used. Arc-length control is one of such relations.
Here, the momentum balance is written as [9]

$$\tilde{r}(\tilde{u}, \lambda) = \tilde{f}_{int}(\tilde{u}) - \lambda \tilde{f}_{ext} = 0 \tag{5.1.1}$$

where $\tilde{f}_{ext}$ is the load pattern applied externally (λ is multiplied with it to define a proportional load) and $\tilde{f}_{int}$ is the internal forces caused by the displacement field $\tilde{u}$. λ is called the load level parameter and is considered as a variable along with u_i, $i = 1$ *to* n. Hence the problem becomes a $(n+1)$ dimensional problem to be solved with Equation 5.1.1 defining only n number of equations.
The $(n+1)^{th}$ equation is obtained from some relation between u_i-s and λ. For arc-length control, this equation turns out to be [9]

$$a = (\Delta\tilde{u}^T \Delta\tilde{u} + \Delta\lambda^2 \Psi^2 \tilde{f}_{ext}^T \tilde{f}_{ext}) - \Delta l^2 = 0 \tag{5.1.2}$$

where Δl is the fixed length of the arc drawn from the current point on the load-displacement curve to get the next equilibrium point on it as shown in Figure 5.2. $\Delta\tilde{u}$ is the total increment in the displacement field and $\Delta\lambda$ is the corresponding increment in the load level parameter. The corresponding iterative increments are expressed by $\delta\tilde{u}$ and $\delta\lambda$. The parameter Ψ is the a scaling parameter between force and displacement. For spherical arc-length method, Ψ is assumed to be 1. Equation 5.1.1 and Equation 5.1.2 can be expanded by Taylor's series about their initial equilibrium configuration 0 and using Equation 5.1.1, as

$$\begin{aligned} \tilde{r}(\tilde{u}, \lambda) = \tilde{r}_0 + \frac{\partial \tilde{r}}{\partial \tilde{u}}\delta\tilde{u} + \frac{\partial \tilde{r}}{\partial \lambda}\delta\lambda = \tilde{r}_0 + \tilde{\tilde{K}}\delta\tilde{u} - \lambda\tilde{f}_{ext} = 0 \; and \\ a = a_0 + 2\Delta\tilde{u}^T\delta\tilde{u} + 2\Delta\lambda\delta\lambda\Psi^2\tilde{f}_{ext}^T\tilde{f}_{ext} = 0 \end{aligned} \tag{5.1.3}$$

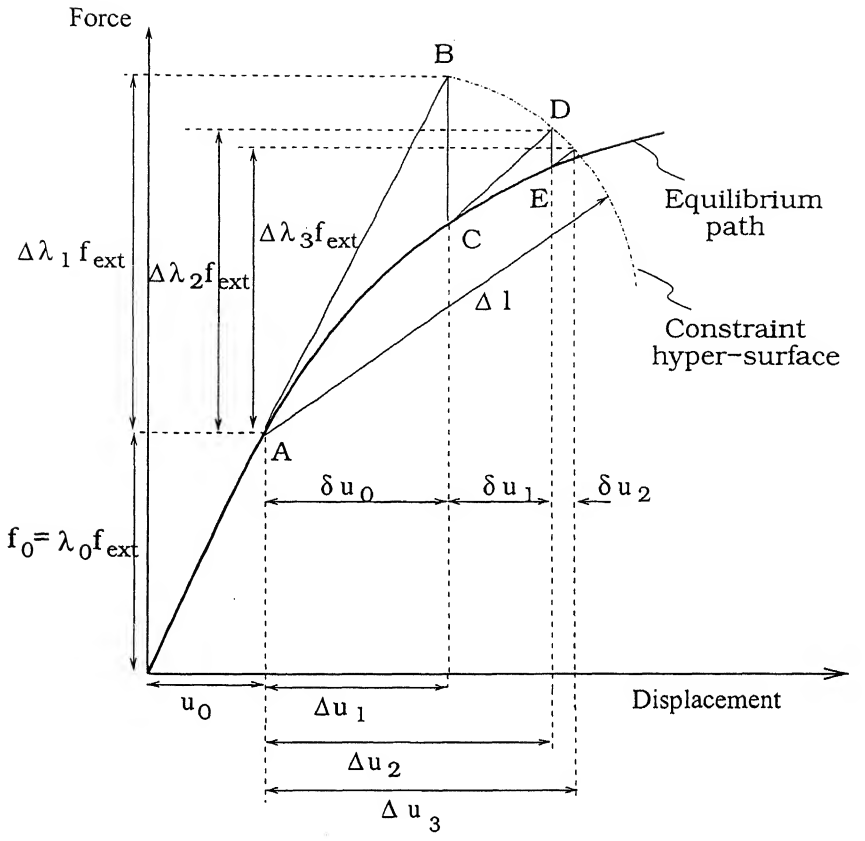

Figure 5.2: Spherical arc-length method

Combining Equation 5.1.3 in a matrix form,

$$\begin{bmatrix} \tilde{\tilde{K}} & -\tilde{f}_{ext} \\ 2\Delta\tilde{u}^T & 2\Delta\lambda\Psi^2\tilde{f}_{ext}^T\tilde{f}_{ext} \end{bmatrix} \begin{Bmatrix} \delta\tilde{u} \\ \delta\lambda \end{Bmatrix} = \begin{Bmatrix} -\tilde{r}_0 \\ -a_0 \end{Bmatrix} \tag{5.1.4}$$

Equation 5.1.4 is often called the **bordered equation** and can be used directly to find $\delta\tilde{u}$ and $\delta\lambda$.

5.2 Spherical arc-length method

In spherical arc-length control method, the basic idea is that the constraint surface is made to be a spherical hyper-surface in (n+1) dimensional plane around the current solution point. The predictor solution as well as the corrector steps for that predictor should be arc-length controlled [10].
Often, the load-displacement scaling parameter Ψ is taken to be one such that the constraint equation represents the equation of a sphere in (n+1) dimension as

$$\Delta\tilde{u}^T\Delta\tilde{u} + \Delta\lambda^2\tilde{f}_{ext}^T\tilde{f}_{ext} = \Delta l^2 \tag{5.2.1}$$

This constraint equation, along with the iterative incremental momentum equation, is arranged in the matrix form as Equation 5.1.4 and solved for the δu-s and $\delta\lambda$. Then the next increment step is calculated as

$$\begin{aligned} \Delta\tilde{u}_{i+1} &= \Delta\tilde{u}_i + \delta\tilde{u}_i \\ \Delta\lambda_{i+1} &= \Delta\lambda_i + \delta\lambda_i \end{aligned} \tag{5.2.2}$$

One of the problems encountered in spherical arc length method is that the constraint surface in Equation 5.2.1 is quadratic in $\Delta\lambda$ and has two possible roots for it satisfying the momentum balance as shown in Figure 5.3. The correct one has to be chosen to prevent doubling back of the solution. This is done by keeping track of the angle of the old increment and comparing the direction difference of it with the two possible solutions from constraint equation. The one with minimum angle with the previous increment can be chosen to prevent doubling back of the result [10]. This situation is shown

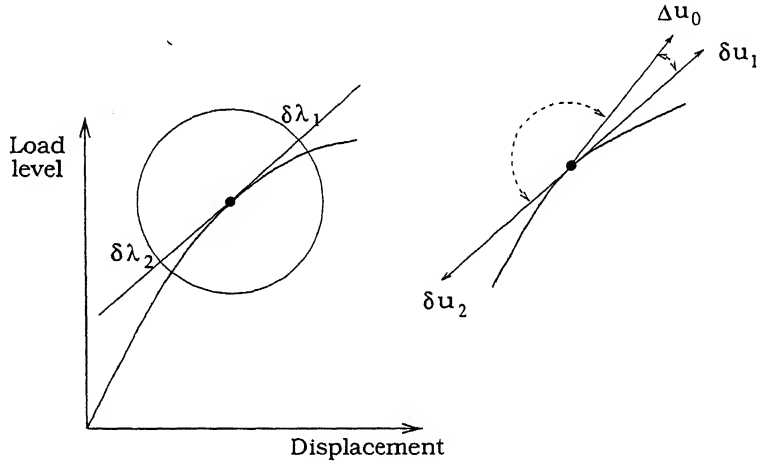

Figure 5.3: Avoiding a solution doubling back

in Figure 5.3. For the case shown, the solution $\{\delta\tilde{u}_1, \delta\lambda_1\}$ is the solution which ensures no doubling back as it has the minimum angle with the previous increment $\Delta\tilde{u}$ direction.
But in case of snap-back, the doubling back of the solution is a desired phenomenon. For that case, one possible method to find out the correct value of $\delta\lambda$, is the minimum residue criteria [10].
To detect that whether the solution is near to the limit point or not, the current stiffness parameter may be used [9]. This is nothing but the ratio of the current tangent stiffness to the initial tangent stiffness. It gives a rough idea about the slope of the load-displacement curve at the current solution point.

5.3 Linearized arc-length method

The spherical constraint Equation 5.1.3 can be linearized by considering $a_0 = 0$, i.e the constraint condition to be satisfied initially [9].

$$2\Delta\tilde{u}^T\delta\tilde{u} + 2\Delta\lambda\delta\lambda\tilde{f}_{ext}^T\tilde{f}_{ext} = 0$$

or,

$$\delta\lambda = -\frac{\Delta\tilde{u}^T\delta\tilde{u}}{\Delta\lambda\tilde{f}_{ext}^T\tilde{f}_{ext}} \tag{5.3.1}$$

This constraint, if arranged in proper manner is nothing but

$$\frac{\Delta\tilde{u}^T\,\Delta\lambda\tilde{f}_{ext}^T}{\Delta\tilde{u}^T\Delta\tilde{u}} \times \frac{\delta\tilde{u}^T\,\delta\lambda\tilde{f}_{ext}^T}{\delta\tilde{u}^T\delta\tilde{u}} = -1$$

i.e. the iterative incremental solution space $\{\delta\tilde{u}, \delta\lambda\}$ is orthogonal to $\{\Delta\tilde{u}, \Delta\lambda\}$.
Two different corrector algorithms based on this linearized arc-length method is shown in Figure 5.4. Figure 5.4(a) shows the Riks-Wempner scheme. Here, the corrector solution $\{\delta\tilde{u}, \delta\lambda\}$ is orthogonal to

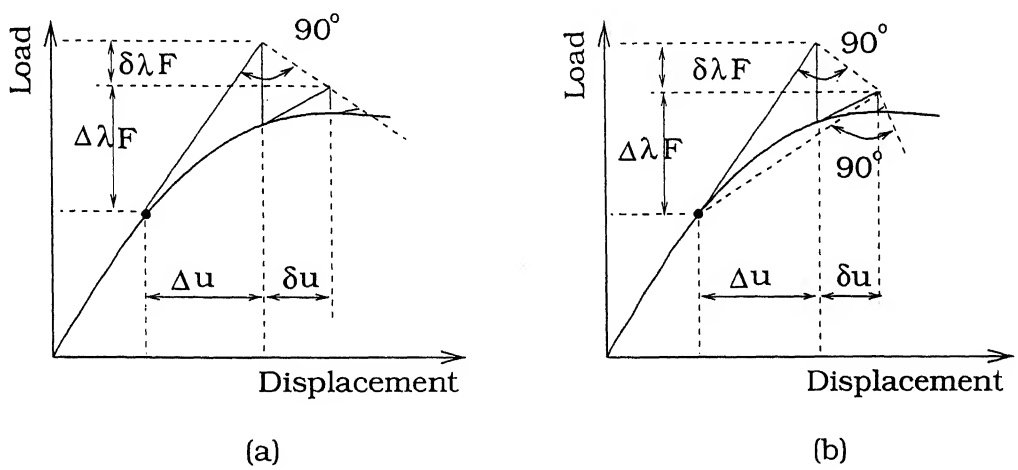

Figure 5.4: Linearized arc-length methods: (a) Riks-Wempner method, (b) Ramm's method

the predictor solution $\{\Delta\tilde{u}, \Delta\lambda\}$. And Figure 5.2(b) shows Ramm's method in which the predictor step $\{\Delta\tilde{u}, \Delta\lambda\}$ is continuously updated and the corrector solution is orthogonal to the secant change [16]. The momentum balance along with the linearized arc-length method can be arranged in matrix form as

$$\begin{bmatrix} \tilde{\tilde{K}} & -\tilde{f}_{ext} \\ \Delta\tilde{u}^T & \Delta\lambda\tilde{f}_{ext}^T\tilde{f}_{ext} \end{bmatrix} \begin{Bmatrix} \delta\tilde{u} \\ \delta\lambda \end{Bmatrix} = \begin{Bmatrix} -\tilde{r}_0 \\ 0 \end{Bmatrix} \tag{5.3.2}$$

5.4 Cylindrical arc-length method

This method was introduced by Crisfield in 1981 [9, 16]. He modified the spherical arc-length method by putting $\Psi = 0$ in Equation 5.1.2. That makes the constraint surface a cylindrical one with its axis along the direction of load parameter λ as

$$\Delta\tilde{u}^T \Delta\tilde{u} = \Delta l^2 \tag{5.4.1}$$

While controlling the arc-length keeping a specific displacement component fixed instead of the whole displacement field, this method reduces to the simple displacement control method and has the disadvantage mentioned at the starting of this chapter.
But this method is a very simple one and can be readily implemented in any computer program. The problems of line search, finding the feasible solution between etc are not issues as they are in spherical arc length control. Hence, this method is used to predict limit point behavior of some structure using the code.

Chapter 6

Discretization

While discretizing the equations by Finite Elements and Finite Difference, the material co-ordianate is considered for spatial discretization. The displacement field $\tilde{u}(\tilde{x}, t)$, being the primary variable, is expressed in a semi-discrete manner by separation of time and space variables as [4, 3]

$$\begin{aligned} \tilde{u}(\tilde{x}, t) &= \tilde{\tilde{\Phi}}_s(\tilde{x})\tilde{u}^e(t) \\ &= \tilde{\tilde{\Phi}}_m(\tilde{X})\tilde{u}^e(t) \end{aligned} \tag{6.0.1}$$

where $\tilde{\tilde{\Phi}}$ is some interpolation function and suffices s and m denotes the spatial and material functions, respectively.

6.1 Discretization in space

In finite elcment discretization, a Lagrangian mesh is considered, and the corresponding approximation is taken by isoparametric assumption as

$$\begin{aligned} \tilde{x} &= \tilde{\tilde{\Phi}}(\tilde{X})\tilde{x}^e(t) \\ \tilde{u} &= \tilde{\tilde{\Phi}}(\tilde{X})\tilde{u}^e(t) \end{aligned} \tag{6.1.1}$$

where $\tilde{\tilde{\Phi}}(\tilde{X})$ is the shape function matrix.
Hence, the virtual displacement field can be discretized as

$$\delta\tilde{u} = \tilde{\tilde{\Phi}}(\tilde{X})\delta\tilde{u}^e \tag{6.1.2}$$

The incremental parameters as

$$\Delta\tilde{u} = \tilde{\tilde{\Phi}}(\tilde{X})\Delta\tilde{u}^e \tag{6.1.3}$$

and time derivatives as

$$\begin{aligned}\dot{\tilde{u}} &= \tilde{\tilde{\Phi}}(\tilde{X})\dot{\tilde{u}}^e \\ \ddot{\tilde{u}} &= \tilde{\tilde{\Phi}}(\tilde{X})\ddot{\tilde{u}}^e \\ \Delta\dot{\tilde{u}} &= \tilde{\tilde{\Phi}}(\tilde{X})\Delta\dot{\tilde{u}}^e \\ \Delta\ddot{\tilde{u}} &= \tilde{\tilde{\Phi}}(\tilde{X})\Delta\ddot{\tilde{u}}^e\end{aligned} \tag{6.1.4}$$

and the deformation gradient is then given as

$$\begin{aligned}\tilde{\tilde{F}} &= \frac{\partial\tilde{x}}{\partial\tilde{X}} \\ &= \frac{\partial\tilde{\tilde{\Phi}}(\tilde{X})}{\partial\tilde{X}}\tilde{x}^e\end{aligned} \tag{6.1.5}$$

6.1.1 Dynamic forces

From Equation 6.1.1 and Equation 6.1.4, the dynamic part of Equation 3.2.10 becomes

$$\begin{aligned}\int_{\mathcal{B}_t}\rho_t\Delta\ddot{\tilde{u}}\cdot\delta\tilde{u}d\Omega &= \int_{\mathcal{B}_t}\rho_t\delta\tilde{u}^T\Delta\ddot{\tilde{u}}d\Omega \\ &= \int_{\mathcal{B}_t}\rho_t\delta\tilde{u}^{eT}\tilde{\tilde{\Phi}}^T\tilde{\tilde{\Phi}}\Delta\ddot{\tilde{u}}^e d\Omega \\ &= \delta\tilde{u}^{eT}\{\int_{\mathcal{B}_t}\rho_t\tilde{\tilde{\Phi}}^T\tilde{\tilde{\Phi}}d\Omega\}\Delta\ddot{\tilde{u}}^e\end{aligned}$$

i.e

$$\int_{\mathcal{B}_t}\rho_t\Delta\ddot{\tilde{u}}\cdot\delta\tilde{u}d\Omega = \delta\tilde{u}^{eT}\tilde{\tilde{M}}\Delta\ddot{\tilde{u}}^e \tag{6.1.6}$$

where $\tilde{\tilde{M}} = \int_{\mathcal{B}_t}\rho_t\tilde{\tilde{\Phi}}^T\tilde{\tilde{\Phi}}d\Omega$ is known as the **mass matrix**.

6.1.2 External forces

From Equation 3.2.10, the external body force part can be discretized as

$$\begin{aligned}\int_{\mathcal{B}_t}\rho_t\Delta\tilde{b}\cdot\delta\tilde{u}d\Omega &= \int_{\mathcal{B}_t}\rho_t\delta\tilde{u}^T\Delta\tilde{b}d\Omega \\ &= \int_{\mathcal{B}_t}\rho_t\delta\tilde{u}^{eT}\tilde{\tilde{\Phi}}^T\tilde{\tilde{\Phi}}\Delta\tilde{b}^e d\Omega \\ &= \delta\tilde{u}^{eT}\{\int_{\mathcal{B}_t}\rho_t\tilde{\tilde{\Phi}}^T\tilde{\tilde{\Phi}}\Delta\tilde{b}^e\}d\Omega\end{aligned}$$

i.e

$$\int_{\mathcal{B}_t}\rho_t\Delta\tilde{b}\cdot\delta\tilde{u}d\Omega = \delta\tilde{u}^{eT}\tilde{f}_b \tag{6.1.7}$$

where $\tilde{f}_b = \int_{\mathcal{B}_t} \rho_t \tilde{\tilde{\Phi}}^T \tilde{\tilde{\Phi}} \Delta\tilde{b}^e d\Omega$ is the discretized external force vector.
And the surface force

$$\begin{aligned}\int_{\partial\mathcal{B}_t} \Delta\tilde{T} \cdot \delta\tilde{u} dS &= \int_{\partial\mathcal{B}_t} \delta\tilde{u}^T \Delta\tilde{T} dS \\ &= \delta\tilde{u}^{eT} \int_{\partial\mathcal{B}_t} \{\tilde{\tilde{\Phi}}_s^T \tilde{\tilde{\Phi}}_s \Delta\tilde{T}^e\} d\Omega\end{aligned}$$

i.e

$$\int_{\partial\mathcal{B}_t} \Delta\tilde{T} \cdot \delta\tilde{u} dS = \delta\tilde{u}^{eT} \tilde{f}_s \tag{6.1.8}$$

where $\tilde{\tilde{\Phi}}_s$ is the shape function matrix for the boundary elements and $\tilde{f}_s = \int_{\partial\mathcal{B}_t} \{\tilde{\tilde{\Phi}}_s^T \tilde{\tilde{\Phi}}_s \Delta\tilde{T}^e\} d\Omega$ is the discretized surface force vector.
Hence the total external force is discretized as

$$\int_{\mathcal{B}_t} \rho_t \Delta\tilde{b} \cdot \delta\tilde{u} d\Omega + \int_{\partial\mathcal{B}_t} \Delta\tilde{T} \cdot \delta\tilde{u} dS = \delta\tilde{u}^{eT}(\tilde{f}_b + \tilde{f}_s) = \delta\tilde{u}^{eT}(\Delta\tilde{f}) \tag{6.1.9}$$

where $\Delta\tilde{f} = \tilde{f}_b + \tilde{f}_s$, is the total incremental external force.

6.1.3 Internal forces

The incremental stress tensor in Equation 3.2.10, expressed by the Jaumann-Zaremba rate increment mentioned in Section 3.3, is

$$\begin{aligned}\Delta\tilde{\tilde{\sigma}} &= \dot{\tilde{\tilde{\sigma}}}_t\Big|_m + \tilde{\tilde{W}}\tilde{\tilde{\sigma}}_t + \tilde{\tilde{\sigma}}_t\tilde{\tilde{W}}^T \\ &= \tilde{\tilde{\tilde{E}}}\tilde{\tilde{D}} + \tilde{\tilde{W}}\tilde{\tilde{\sigma}}_t + \tilde{\tilde{\sigma}}_t\tilde{\tilde{W}}^T\end{aligned}$$

First, the incremental part of $\tilde{\tilde{\sigma}}$ for stretch is considered. The corresponding virtual work is

$$\begin{aligned}\Delta\tilde{\tilde{\sigma}} : \frac{\partial\delta\tilde{u}}{\partial\tilde{x}} &= \Delta\tilde{\tilde{\sigma}} : \delta(\tilde{\tilde{D}} + \tilde{\tilde{W}}) \\ &= \Delta\tilde{\tilde{\sigma}} : \delta\tilde{\tilde{D}} \qquad \text{(as } \tilde{\tilde{W}} \text{ is skew and } \Delta\tilde{\tilde{\sigma}} \text{ is symmetric)} \\ &= (\tilde{\tilde{\tilde{E}}}\tilde{\tilde{D}} + \tilde{\tilde{W}}\tilde{\tilde{\sigma}}_t + \tilde{\tilde{\sigma}}_t\tilde{\tilde{W}}^T) : \delta\tilde{\tilde{D}}\end{aligned}$$

That implies [10]

$$\int_{\mathcal{B}_t} \Delta\tilde{\tilde{\sigma}} : \frac{\partial\delta\tilde{u}}{\partial\tilde{x}} d\Omega = \int_{\mathcal{B}_t} (\tilde{\tilde{\tilde{E}}}\tilde{\tilde{D}} : \delta\tilde{\tilde{D}} + 2\tilde{\tilde{\sigma}}_t\tilde{\tilde{W}}^T : \delta\tilde{\tilde{D}}) d\Omega^1 \tag{6.1.10}$$

For discrezitation, the two matrices need to be expressed in Voigt notation, or in other words, in a vector form such that the balance equations remain the same.

[1] if $a, b \in \mathcal{R}_{sym}$ and $w \in \mathcal{R}_{skew}$, then $wa : b = tr(aw^T b) = -tr(awb) = -a_{ik}w_{kj}b_{ij} = w_{ik}a_{kj}b_{ij} = aw^T : b$

Conventionally, the stress matrix

$$\begin{bmatrix} \sigma_{xx} & \sigma_{xy} & \sigma_{xz} \\ \sigma_{yx} & \sigma_{yy} & \sigma_{yz} \\ \sigma_{zx} & \sigma_{zy} & \sigma_{zz} \end{bmatrix}$$

is written in vector form by the Voigt rule for symmetric kinetic tensors[4] as

$$\{\sigma_{voigt}\} = \{\sigma_{xx}\ \sigma_{yy}\ \sigma_{zz}\ \sigma_{yz}\ \sigma_{xz}\ \sigma_{xy}\}^T \tag{6.1.11}$$

And from Viogt rule for second order symmetric kinematic tensor, the deformation tensor

$$\begin{bmatrix} D_{xx} & D_{xy} & D_{xz} \\ D_{yx} & D_{yy} & D_{yz} \\ D_{zx} & D_{zy} & D_{zz} \end{bmatrix}$$

is arranged in vector form as

$$\{D_{voigt}\} = \{D_{xx}\ D_{yy}\ D_{zz}\ 2D_{yz}\ 2D_{xz}\ 2D_{xy}\}^T \tag{6.1.12}$$

such that,

$$\tilde{\tilde{\sigma}} : \tilde{\tilde{D}} = \tilde{\sigma}_{voigt} \cdot \tilde{D}_{voigt}$$

Now, the as the spin tensor is not a symmetric one, the conventional Voigt rules cannot be applied to transfer them into vector notation. Rather, the corresponding virtual work is expanded as follows,

$$\begin{aligned} \tilde{\tilde{\sigma}}\tilde{\tilde{W}}^T : \delta\tilde{\tilde{D}} &= tr\left[\tilde{\tilde{W}}\tilde{\tilde{\sigma}}(\delta\tilde{\tilde{D}})\right] \\ &= tr\left[\tilde{\tilde{\sigma}}(\delta\tilde{\tilde{D}})\tilde{\tilde{W}}\right] \\ &= (\delta\tilde{\tilde{D}})\tilde{\tilde{\sigma}} : \tilde{\tilde{W}} \end{aligned} \tag{6.1.13}$$

$$\text{Now, say } (\delta\tilde{\tilde{D}})\tilde{\tilde{\sigma}}_t = \begin{bmatrix} a_{11} & a_{12} & a_{13} \\ a_{21} & a_{22} & a_{23} \\ a_{31} & a_{32} & a_{33} \end{bmatrix}, \text{ and } \tilde{\tilde{W}} = \begin{bmatrix} 0 & \alpha & \beta \\ -\alpha & 0 & \gamma \\ -\beta & -\gamma & 0 \end{bmatrix} \tag{6.1.14}$$

Then

$$[\delta D][\sigma_t] : [W] = \begin{bmatrix} a_{11} & a_{12} & a_{13} \\ a_{21} & a_{22} & a_{23} \\ a_{31} & a_{32} & a_{33} \end{bmatrix} : \begin{bmatrix} 0 & \alpha & \beta \\ -\alpha & 0 & \gamma \\ -\beta & -\gamma & 0 \end{bmatrix}$$
$$= tr\left(\begin{bmatrix} a_{11} & a_{21} & a_{31} \\ a_{12} & a_{22} & a_{32} \\ a_{13} & a_{23} & a_{33} \end{bmatrix} \begin{bmatrix} 0 & \alpha & \beta \\ -\alpha & 0 & \gamma \\ -\beta & -\gamma & 0 \end{bmatrix} \right)$$
$$= \alpha(a_{12} - a_{21}) + \beta(a_{13} - a_{31}) + \gamma(a_{23} - a_{32})$$

Combining this result with Equation 6.1.13 and 6.1.14,

$$\tilde{\tilde{\sigma}}\tilde{\tilde{W}}^T : \delta\tilde{\tilde{D}} = \begin{Bmatrix} (a_{12} - a_{21}) \\ (a_{13} - a_{31}) \\ (a_{23} - a_{32}) \end{Bmatrix} \cdot \begin{Bmatrix} \alpha \\ \beta \\ \gamma \end{Bmatrix} \tag{6.1.15}$$

Equation 6.1.15 gives the required Voigt vector expression for the rotational part of Equation 6.1.10. Now, expressing the terms by the shape function $[\Phi]$, deformation part of Equation 6.1.10

$$\int_{\mathcal{B}_t} \tilde{\tilde{E}}\tilde{D} \cdot \delta\tilde{D} d\Omega = \int_{\mathcal{B}_t} \tilde{\tilde{E}}\delta\tilde{D}^T\tilde{D} d\Omega$$
$$= \int_{\mathcal{B}_t} \tilde{\tilde{E}}\delta\tilde{u}^{eT}\tilde{\tilde{B}}^T\tilde{\tilde{B}}\tilde{u}^e d\Omega$$

where $\tilde{\tilde{E}}$ is the material tensor expressed in matrix form by Voigt notation as discussed in Section 3.6 and $\tilde{\tilde{B}}$ is defined as $\tilde{\tilde{D}} = \tilde{\tilde{B}}\Delta\tilde{u}^e$. Then, the internal force for deformation can be discretized as

$$\int_{\mathcal{B}_t} \tilde{\tilde{E}}\tilde{D} \cdot \delta\tilde{D} d\Omega = \delta\tilde{u}^{eT}\tilde{\tilde{K}}_D\Delta\tilde{u}^e \tag{6.1.16}$$

where $\tilde{\tilde{K}}_D = \int_{\mathcal{B}_t} \tilde{\tilde{E}}\tilde{\tilde{B}}^T\tilde{\tilde{B}} d\Omega$ is known as the stiffness matrix for the deformation $\tilde{\tilde{D}}$.
And using Equation 6.1.13, 6.1.14 and 6.1.15, the rotational part of Equation 6.1.10 is discretized as

$$\int_{\mathcal{B}_t} 2\tilde{\tilde{\sigma}}_t\tilde{\tilde{W}}^T : \delta\tilde{\tilde{D}} d\Omega = \int_{\mathcal{B}_t} \begin{Bmatrix} (a_{12} - a_{21}) \\ (a_{13} - a_{31}) \\ (a_{23} - a_{32}) \end{Bmatrix}^T \begin{Bmatrix} \alpha \\ \beta \\ \gamma \end{Bmatrix} d\Omega$$
$$= \int_{\mathcal{B}_t} \delta\tilde{u}^{eT}\tilde{\tilde{B}}_1^T\tilde{\tilde{B}}_2\Delta\tilde{u}^e d\Omega$$

where $\tilde{\tilde{B}}_1$ is defined as $\{(a_{12} - a_{21}),\ (a_{13} - a_{31}),\ (a_{23} - a_{32})\}^T = \tilde{\tilde{B}}_1\delta\tilde{u}^e$, and $\tilde{\tilde{B}}_2$ as $\{\alpha,\ \beta,\ \gamma\}^T = \tilde{\tilde{B}}_2\Delta\tilde{u}^e$.

Hence, the rotational part is

$$\int_{\mathcal{B}_t} 2\tilde{\tilde{\sigma}}_t \tilde{\tilde{W}}^T : \delta\tilde{\tilde{D}} d\Omega = \delta\tilde{u}^{eT} \tilde{\tilde{K}}_W \Delta\tilde{u}^e \tag{6.1.17}$$

where $\tilde{\tilde{K}}_W = \int_{\mathcal{B}_t} \tilde{\tilde{B}}_1^T \tilde{\tilde{B}}_2 d\Omega$, is the stiffness matrix for the rotational parts, or the geometric stiffness matrix of the structure.

So, the total virtual work done by the internal forces is

$$\int_{\mathcal{B}_t} \Delta\tilde{\tilde{\sigma}} : \frac{\partial\delta\tilde{u}}{\partial\tilde{x}} d\Omega = \delta\tilde{u}^{eT} \tilde{\tilde{K}} \Delta\tilde{u}^e \tag{6.1.18}$$

where $\tilde{\tilde{K}} = \tilde{\tilde{K}}_D + \tilde{\tilde{K}}_W$ is the total stiffness matrix of the system.

6.1.4 Expressions of different matrices used for discretization

Say, the primary unknowns $\{u_1,\ u_2,\ u_3\}$ at any generic point is interpolated as

$$\begin{aligned} u_1 &= N_1 u_1^{e1} + N_2 u_1^{e2} + ... + N_{nn} u_1^{e\ nn} \\ u_2 &= N_1 u_2^{e1} + N_2 u_2^{e2} + ... + N_{nn} u_2^{e\ nn} \\ and\ u_3 &= N_1 u_3^{e1} + N_2 u_3^{e2} + ... + N_{nn} u_3^{e\ nn} \end{aligned}$$

Or,

$$\begin{Bmatrix} u_1 \\ u_2 \\ u_3 \end{Bmatrix} = \begin{bmatrix} N_1 & 0 & 0 & N_2 & 0 & 0 & ..... & N_{nn} & 0 & 0 \\ 0 & N_1 & 0 & 0 & N_2 & 0 & ..... & 0 & N_{nn} & 0 \\ 0 & 0 & N_1 & 0 & 0 & N_2 & ..... & 0 & 0 & N_{nn} \end{bmatrix} \begin{Bmatrix} u_1^{e1} \\ u_2^{e1} \\ u_3^{e1} \\ ... \\ u_1^{e\ nn} \\ u_2^{e\ nn} \\ u_3^{e\ nn} \end{Bmatrix}$$

Hence the shape function matrix is given by

$$[\Phi] = \begin{bmatrix} N_1 & 0 & 0 & N_2 & 0 & 0 & ..... & N_{nn} & 0 & 0 \\ 0 & N_1 & 0 & 0 & N_2 & 0 & ..... & 0 & N_{nn} & 0 \\ 0 & 0 & N_1 & 0 & 0 & N_2 & ..... & 0 & 0 & N_{nn} \end{bmatrix} \tag{6.1.19}$$

The rate of deformation tensor (in Voigt notation) can be expressed as

$$\begin{Bmatrix} D_{11} \\ D_{22} \\ D_{33} \\ D_{23} \\ D_{13} \\ D_{12} \end{Bmatrix} = \begin{Bmatrix} \frac{\partial \Delta u_1}{\partial x_1} \\ \frac{\partial \Delta u_2}{\partial x_2} \\ \frac{\partial \Delta u_3}{\partial x_3} \\ \frac{\partial \Delta u_2}{\partial x_3} + \frac{\partial \Delta u_3}{\partial x_2} \\ \frac{\partial \Delta u_1}{\partial x_3} + \frac{\partial \Delta u_3}{\partial x_1} \\ \frac{\partial \Delta u_1}{\partial x_2} + \frac{\partial \Delta u_2}{\partial x_1} \end{Bmatrix} = [B]\{\Delta u\}$$

i.e.

$$[B] = \begin{bmatrix} \Phi_{11,x1} & \Phi_{12,x1} & .... & \Phi_{1\ nn,x1} \\ \Phi_{21,x2} & \Phi_{22,x2} & .... & \Phi_{2\ nn,x2} \\ \Phi_{31,x3} & \Phi_{32,x3} & .... & \Phi_{3\ nn,x3} \\ \Phi_{21,x3}+\Phi_{31,x2} & \Phi_{22,x3}+\Phi_{32,x2} & .... & \Phi_{2\ nn,x3}+\Phi_{3\ nn,x2} \\ \Phi_{11,x3}+\Phi_{31,x1} & \Phi_{12,x3}+\Phi_{32,x1} & .... & \Phi_{1\ nn,x3}+\Phi_{3\ nn,x1} \\ \Phi_{11,x2}+\Phi_{21,x1} & \Phi_{12,x2}+\Phi_{22,x1} & .... & \Phi_{1\ nn,x2}+\Phi_{2\ nn,x1} \end{bmatrix} \tag{6.1.20}$$

Similarly, the other strain displacement matrix, for rotation, can be written as

$$[B_2] = \frac{1}{2}\begin{bmatrix} N_{1,x2} & -N_{1,x1} & 0 & N_{2,x2} & -N_{2,x1} & 0 & ... & N_{nn,x2} & -N_{nn,x1} & 0 \\ N_{1,x3} & 0 & -N_{1,x1} & N_{2,x3} & 0 & -N_{2,x1} & ... & N_{nn,x3} & 0 & -N_{nn,x1} \\ 0 & N_{1,x3} & -N_{1,x2} & 0 & N_{2,x3} & -N_{2,x2} & ... & 0 & N_{nn,x3} & -N_{nn,x2} \end{bmatrix} \tag{6.1.21}$$

And now combining the Equations 6.1.6, 6.1.9 and 6.1.18, the incremental virtual work statement can be arranged as

$$\delta\tilde{u}^{eT}\tilde{\tilde{M}}\Delta\ddot{\tilde{u}}^e + \delta\tilde{u}^{eT}\tilde{\tilde{K}}\Delta\tilde{u}^e = \delta\tilde{u}^{eT}\Delta\tilde{f}$$

As $\delta\tilde{u}$ is an arbitrary virtual displacement, the discretized momentum balance is

$$[M]\{\Delta\ddot{u}^e\} + [K]\{\Delta u^e\} = \{\Delta f\} \tag{6.1.22}$$

6.1.5 Discretized heat transfer equations

The temperature field is assumed to be interpolated as

$$\theta = N_1\theta_1^e + N_2\theta_2^e + ... + N_{nn}\theta_{nn}^e$$
$$or,\ \theta = \{\Phi_1\}^T\{\theta^e\}$$

Then

$$\begin{aligned}\delta\theta &= \{\Phi_1\}^T\{\delta\theta^e\}\\ \Delta\theta &= \{\Phi_1\}^T\{\Delta\theta^e\}\\ \Delta\dot{\theta} &= \{\Phi_1\}^T\{\Delta\dot{\theta}^e\}\ and\\ \Delta\theta_{,i} &= \{\Phi_{1,i}\}^T\{\Delta\theta^e\}\end{aligned} \tag{6.1.23}$$

Now, the incremental energy balance equation for heat transfer (Equation 3.5.5) can be discretized similar to its elastic counterpart as

$$\int_{\mathcal{B}_t} c\rho\{\delta\theta^e\}^T\{\Phi_1\}\{\Phi_1\}^T\{\Delta\dot{\theta}^e\}d\Omega + \int_{\mathcal{B}_t}\left(k_i\{\delta\theta^e\}^T\{\Phi_{1,i}\}\{\Phi_{1,i}\}^T\{\Delta\theta^e\}\right)d\Omega = \int_{\mathcal{B}_t}\{\delta\theta^e\}^T\{\Phi_1\}\{\Phi_1\}^T\{q^{be}\}d\Omega + \{q_s\}$$

Or,

$$\{\delta\theta^e\}^T\left([C_{th}]\{\Delta\dot{\theta}^e\} + [K_{th}]\{\Delta\theta^e\}\right) = \{\delta\theta^e\}^T\{\Delta q\}$$

where $[C_{th}] = \int_{\mathcal{B}_t} c\rho\{\Phi_1\}\{\Phi_1\}^T d\Omega$, and $[K_{th}] = \int_{\mathcal{B}_t}\left(k_i\{\delta\theta^e\}^T\{\Phi_{1,i}\}\right)d\Omega,\ i = 1,2,3$ and $\{\Delta q\} = \int_{\mathcal{B}_t}\{\Phi_1\}\{\Phi_1\}^T\{q^{be}\}d\Omega + \{q_s\}$, $\{q_s\}$ being the heat flux through the boundary. Again, as $\{\delta\theta^e\}$ can be chosen arbitrarily, the discretized heat flux balance can be written as

$$[C_{th}]\{\Delta\dot{\theta}^e\} + [K_{th}]\{\Delta\theta^e\} = \{\Delta q\} \tag{6.1.24}$$

6.2 Discretization of the contact constraint

This work includes just the sticking contact of the body against a rigid wall. For that case, the penetration function for the Lagrangian multiplier formulation in Section 4.2 becomes

$$\tilde{g} = \tilde{u}_{contact}$$

where $\tilde{u}_{contact}$ are the displacement fields at the contacting nodes. These contacting nodes are a subset of all the nodes and the penetration function can be written as

$$\begin{aligned}\{g\} &= [\hat{C}]\{u^e\}\\ where\ \hat{C}_{ij} &= \begin{cases}1 & if\ u_j\ is\ the\ i^{th}\ contacting\ d.o.f\\ 0 & otherwise\end{cases}\end{aligned} \tag{6.2.1}$$

And also,

$$\{\delta g\} = [\hat{C}]\{\delta u^e\}$$
$$and\ \{\Delta g\} = [\hat{C}]\{\Delta u^e\}$$

Then Equation 4.2.5 can be discretzed as

$$\{\delta u^e\}^T[M]\{\Delta\ddot{u}^e\} + \{\delta u^e\}^T[K]\{\Delta u^e\} - \{\delta u^e\}^T\{\Delta f_{ext}\} - \left(\{\delta u^e\}^T[\hat{C}]^T\{\Delta\lambda\} + \{\delta\lambda\}^T[\hat{C}]\{\Delta u^e\}\right) = 0$$

Or,

$$\{\delta u^e\}^T\left([M]\{\Delta\ddot{u}^e\} + [K]\{\Delta u^e\} - \{\Delta f_{ext}\} - [\hat{C}]^T\{\Delta\lambda\}\right) = 0$$
$$and\ \{\delta\lambda\}^T[\hat{C}]\{\Delta u^e\} = 0$$

where λ is the contact forces at the contact nodes.
As both the virtual fields $\{\delta u^e\}$ and $\{\lambda\}$ can be chosen arbitrary, the momentum balance turns out to be

$$\begin{aligned}[M]\{\Delta\ddot{u}^e\} + [K]\{\Delta u^e\} - [\hat{C}]^T\{\Delta\lambda\} = \{\Delta f_{ext}\}\ and \\ [\hat{C}]\{\Delta u^e\} = 0\end{aligned} \tag{6.2.2}$$

Equation 6.2.2 can be combined to be arranged in form as

$$\begin{bmatrix}[M] & [0]\\ [0] & [0]\end{bmatrix}\begin{Bmatrix}\{\Delta\ddot{u}^e\}\\ \{\Delta\ddot{\lambda}\}\end{Bmatrix} + \begin{bmatrix}[K] & -[\hat{C}]^T\\ [\hat{C}] & [0]\end{bmatrix}\begin{Bmatrix}\{\Delta u^e\}\\ \{\Delta\lambda\}\end{Bmatrix} = \begin{Bmatrix}\{\Delta f_{ext}\}\\ \{0\}\end{Bmatrix} \tag{6.2.3}$$
$$or\ [\mathbf{M_{contact}}]\{\mathbf{\Delta\ddot{u}'}\} + [\mathbf{K_{contact}}]\{\mathbf{\Delta u'}\} = \{\mathbf{\Delta f'}\}$$

where $\{\Delta u'\} = \{\{\Delta u^e\}, \{\Delta\lambda\}\}$ and $\{\Delta f'\} = \{\{\Delta f_{ext}\}, \{0\}\}$.

6.3 Discretization in time

Conventionally, two types of methods are used for time integration scheme of Equation 6.1.22. Namely, **explicit** and **implicit time integration scheme**.
Explicit schemes are based on the idea that equilibrium vales are known at time t, and they are used to obtain the solution at time $t+\Delta t$ [4, 17]. As the name suggests, this scheme is a rather direct method to integrate the time dynamic equation and no prior transformation is done before integration [3]. Though the explicit integration schemes like Central difference scheme, are very popular and simple to apply, they have one disadvantage that they are conditionally stable [17].
The implicit schemes of numerical integration, on the other hand, are unconditionally stable. They depend on the values of the variable and its derivatives in both time steps t and $t+\Delta t$. One of the most

popular methods in implicit schemes is the Newmark-β method. This method is often interpreted as the extension of linear acceleration method [3]. The assumptions in this method are

$$\tilde{u}_{t+\Delta t} = \tilde{u}_t + \dot{\tilde{u}}_t \Delta t + \left[(\frac{1}{2} - \alpha) \ddot{\tilde{u}}_t + \alpha \ddot{\tilde{u}}_{t+\Delta t} \right] \Delta t^2 \tag{6.3.1}$$

and

$$\dot{\tilde{u}}_{t+\Delta t} = \dot{\tilde{u}}_t + \left[(1 - \delta) \ddot{\tilde{u}}_t + \delta \ddot{\tilde{u}}_{t+\Delta t} \right] \Delta t \tag{6.3.2}$$

where α and δ are Newmark constants whose values dictates the dependency between the values and slopes at time t and $t + \Delta t$. In this work, the constant acceleration method, or the trapezoidal rule is

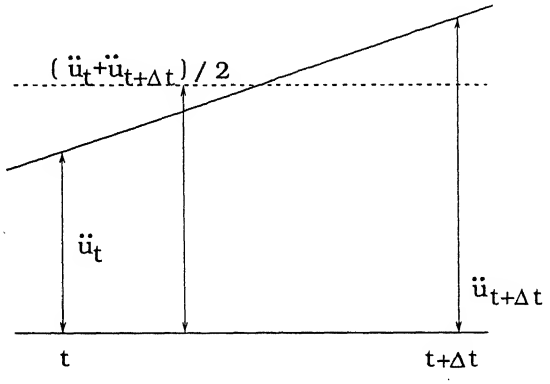

Figure 6.1: Constant average acceleration Newmark scheme

used for which $\alpha = \frac{1}{4}$ and $\delta = \frac{1}{2}$. This scheme is shown in Figure 6.1. This method is unconditionally stable and was originally proposed by Newmark [3].

6.3.1 Modification of discretized equations for Newmark integration scheme

From Equation 6.3.1,

$$\Delta \ddot{\tilde{u}} = \dot{\tilde{u}}_t \Delta t + \left[(\frac{1}{2} - \alpha) \ddot{\tilde{u}}_t + \alpha \ddot{\tilde{u}}_{t+\Delta t} \right] \Delta t^2$$

or,

$$\Delta \ddot{\tilde{u}} = \frac{1}{\alpha \Delta t^2} \Delta \tilde{u} - \frac{1}{\alpha \Delta t} \dot{\tilde{u}}_t - \frac{1}{2\alpha} \ddot{\tilde{u}}_t \tag{6.3.3}$$

And from Equation 6.3.2,

$$\Delta \dot{\tilde{u}} = \left[\ddot{\tilde{u}}_t + \delta \Delta \ddot{\tilde{u}} \right] \Delta t$$

Replacing $\Delta \ddot{\tilde{u}}$ from Equation 6.3.3,

$$\Delta \dot{\tilde{u}} = \left[\ddot{\tilde{u}}_t + \frac{\delta}{\alpha \Delta t^2} \Delta \tilde{u} - \frac{\delta}{\alpha \Delta t} \dot{\tilde{u}}_t - \frac{\delta}{2\alpha} \ddot{\tilde{u}}_t \right] \Delta t \tag{6.3.4}$$

Using Equation 6.3.3 and 6.3.4, Equation 6.1.22 can be modified as

$$\begin{aligned} [\hat{\mathbf{K}}]\{\mathbf{\Delta u^e}\} &= \{\mathbf{\Delta \hat{F}}\} \\ where, [\hat{K}] &= [K] + \frac{1}{\alpha \Delta t^2}[M] \\ and\ \{\Delta \hat{f}\} &= \{\Delta f\} + \frac{1}{\alpha \Delta t}[M]\{\dot{u}_t\} + \frac{1}{2\alpha}[M]\{\ddot{u}_t\} \end{aligned} \tag{6.3.5}$$

Similarly, the discretized heat transfer Equation 6.1.24 can be modified using Newmark relation Equation 6.3.4 as

$$\begin{aligned} [\hat{\mathbf{K}}_{\mathbf{th}}]\{\mathbf{\Delta \theta^e}\} &= \{\mathbf{\Delta \hat{q}_{th}}\} \\ where, [\hat{K}_{th}] &= [K_{th}] + \frac{\delta}{\alpha \Delta t}[C_{th}] \\ and\ \{\Delta \hat{q}_{th}\} &= \{\Delta q\} + \frac{\delta}{\alpha}[C_{th}]\{\dot{\theta}_t\} - \left(1 - \frac{\delta}{2\alpha}\right)\Delta t[C_{th}]\{\ddot{\theta}_t\} \end{aligned} \tag{6.3.6}$$

6.3.2 Stability of Newmark-β scheme

As discussed in Cook [13], the accuracy, stability and damping is also a matter of importance while using Newmark-β. The scheme is said to be unconditionally stable for

$$2\alpha = \delta = \frac{1}{2}$$

But as observed from the computational results, often there exists an oscillation in the solution with $\alpha = 0.25$ and $\delta = 0.5$. This oscillation can be reduced using higher values of those constants. But according to Cook, the process reduces the accuracy of the solution. For $\delta > 0.5$, the stability is conditional and the condition on the corresponding time step length is [13]

$$\Delta t \leq \frac{\Omega_{crit}}{\omega_{max}} = \frac{\Omega_{crit} T_{min}}{2\Pi}\ and\ \alpha < \frac{1}{2}\delta$$

where ω_{max} and T_{min} are the highest natural frequency of the structure and corresponding time period. And Ω_{crit} is defined as

$$\Omega_{crit} = \frac{\xi\left(\delta - \frac{1}{2}\right) + \sqrt{\frac{\delta}{2} - \alpha + \xi^2\left(\delta - \frac{1}{2}\right)^2}}{\delta/2 - \alpha}$$

where ξ is the damping ratio. When $\delta > 0.5$, allowable time step length is increased damping.
For $\delta > 0.5$, Newmark method displays algorithmic damping, and according to Cook, the accuracy of the result is reduced. In that case, the right choice of α is $\alpha = \frac{1}{4}\left(\delta + \frac{1}{2}\right)^2$.

Chapter 7

Results and discussion

For checking the theories deduced, a computer program is developed using FORTRAN 90.
Tri-quadratic Lagrangian shape functions are used for spatial finite element discretization and constant acceleration Newmark-β or trapezoidal time integration rule is used for discretization in time. Newton-Raphson scheme is used for the predictor-corrector steps used.
As a first step, some standard and benchmark static problems are solved by UL method in a quasi-static manner (refer Figure 2.7). And for thermo-elastic problems, heat transfer equations are assumed to be decoupled from the elastic equations. First, heat transfer problem is solved independently and then the resulting stresses are fed into the elastic part to solve for the deformation. Then, a few of the continuation techniques are coded to capture some standard unstable phenomena. The contact constraints are also applied and their validity is checked.
But for the dynamic formulation, Newmark-β time integration scheme is used which is unconditionally stable for specific values of the Newmark constants. The condition for the process being unconditionally stable is $2\alpha \geq \delta \geq \frac{1}{2}$ [13]. And for conditional stability, the time step size should be less than some critical size [13].
For the inherent instability and slow convergence rate of Newmark-β scheme, the continuation methods have not been extended to the dynamic cases as they themselves are quite complex regarding the application of Newton-Raphson method near the limit points.
The results have been compared with strength of material solutions and ANSYS results using 20 noded brick elements. The material constants of the structure is taken as shown in Table 7.1

Young's modulus	$2.1\ e^5$
Poisson's ratio	0.3333
Density	$7.8\ e^{-6}$
Thermal conductivity	0.2
Thermal expansion coefficient	$1.0\ e^{-6}$

Table 7.1: Material constants used

7.1 Static analysis

The model used for the static analyses is mainly a uniform rectangular cross section beam / bar as shown in Figure 7.1. For the bending and axial tension, the cross section of the beam is taken as 1 unit X 1 unit and the length is taken as 5 units. For the buckling analysis, the length is taken to be 20 units.

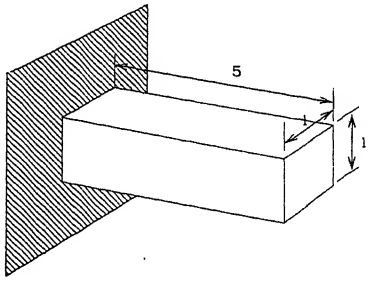

Figure 7.1: Model used for static analysis

7.1.1 Bending of a beam

A distributed flexure load is applied at the free end of the beam models shown. The results, compared to strength of materials(S.O.M) and ANSYS are as follows:

End load	End deflection from S.O.M	End deflection from ANSYS	End deflection from Program
10 units	$2.3810\ e^{-2}$	$2.4027\ e^{-2}$	$2.4011\ e^{-2}$
20 units	$4.7619\ e^{-2}$	$4.8054\ e^{-2}$	$4.7880\ e^{-2}$

Table 7.2: Load vs deflection for bending of a beam for static analysis

From Table 7.2, it can be observed that both the solutions obtained by ANSYS and the program are to some extent softer than the one obtained by strength of materials Euler Bernoulli beam theory. This difference is expected for the constraints imposed on bending by Euler's theorem.

But though the effects of rotation is considered in the program (through Jaumann-Zaremba objective stress rate) the ANSYS results happen to be a little bit softer than the program output. Apparently, this is because of the corner singularities of the beam and the difference in the types of elements used. The code uses 27 noded tri-quadratic Lagrangian element while in ANSYS, the closest element available is the 20 noded serendipity brick elements.

The load-displacement curve for this results is shown in Figure 7.2.

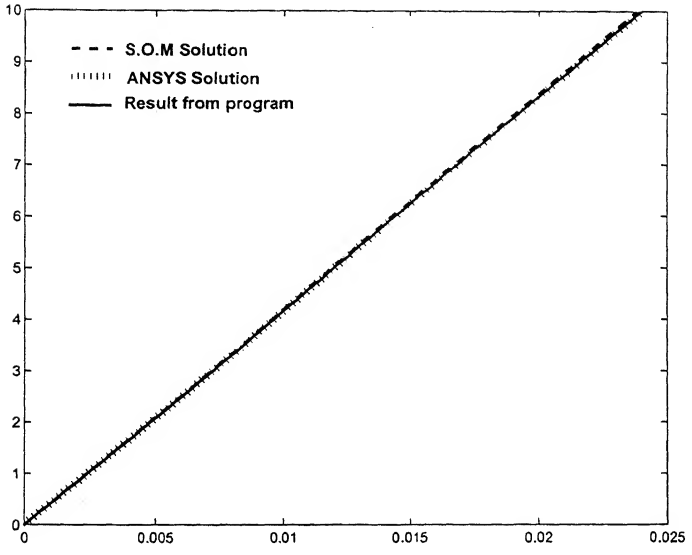

Figure 7.2: Load-deflection curve for bending load

7.1.2 Axial end load applied on a bar

The same model is used as before. A uniformly distributed tensile load is applied at the free end. The corresponding deflections are found as:

End load	End deflection from S.O.M	End deflection from ANSYS	End deflection from Program
50 units	$1.1905\ e^{-3}$	$1.2040\ e^{-3}$	$1.2699\ e^{-3}$
100 units	$2.3810\ e^{-3}$	$2.4080\ e^{-3}$	$2.4930\ e^{-3}$

Table 7.3: Load vs deflection for axial stretch of a bar for static analysis

Table 7.3 shows a clear difference between the strength of material(S.O.M), ANSYS and program solutions for the deflection of the free end under axial tension. The ANSYS solution is a bit softer than the s.o.m solution, and the solution obtained from the program using 10 updated Lagrangian steps is much more softer. This kind of result is expected as updated Lagrangian scheme was used and effect of rotation was taken into account. The plot of these results is shown in Figure 7.3.

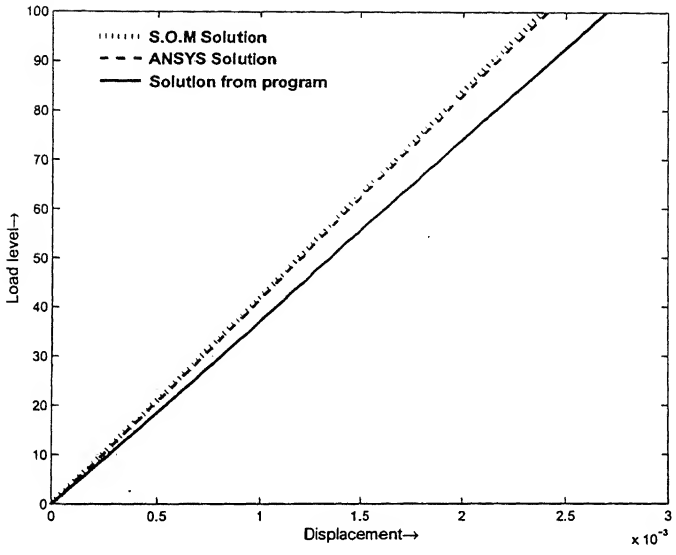

Figure 7.3: Load-deflection curve for axial load

7.1.3 Heat transfer analysis

The thermal balance equation is considered to be decoupled from the elastic one in this analysis. The model used in the previous sections, is taken and a pure thermal load (no force or moment) is applied. The temperature response at the free end of the bar under a uniformly distributed end heat flux is shown in Table 7.4. Here also, the updated Lagrangian steps gives a high numerical value of the free end temperature.

End heat flux	Free end temperature from ANSYS	Free end temperature from Program
10 units	250.0000 K	255.6780 K
20 units	500.0000 K	511.3561 K

Table 7.4: Temperature at the end of a bar with uniform heat flux at the free end

7.2 Application of continuation techniques (static analysis)

The continuation methods, mentioned in Chapter 5, are applied on some standardized models and are compared with the compared with conventional results. The most simple continuation algorithm, the cylindrical arc-length algorithm [9] is used in the program to capture the structural instabilities.

7.2.1 Buckling of a beam

The same model mentioned above is used with a compressive end load. The length of the bar is taken to be 20 units, or rather L/D ration is taken to be 20. As the non-linear balance equations has been

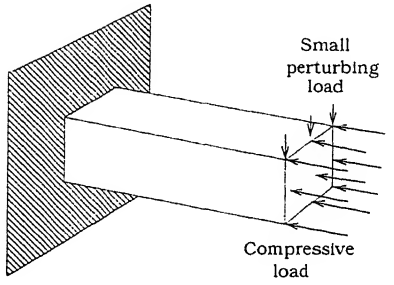

Figure 7.4: Model used for buckling analysis

linearized about the equilibrium configuration, a very small perturbation flexure load should be applied at the end to initiate buckling as shown in Figure 7.4

In Figure 7.5 the result from the cylindrical arc length method is plotted against the critical buckling load obtained from Eulers formula for long columns.

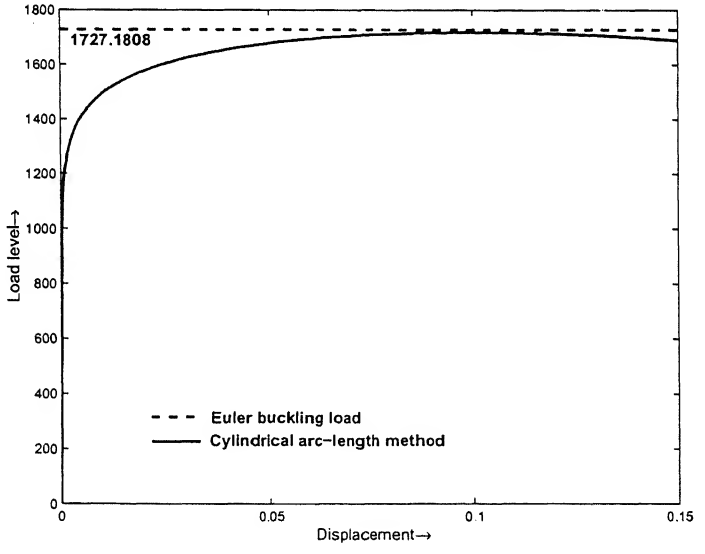

Figure 7.5: Load-displacement curve for buckling of a slender bar

L/D ratio	Critical Euler load	Critical load from program
20	1727.1808	1717.4666 (at 0.1 unit end deflection)

Table 7.5: ANSYS and program solution for buckling load

In the load deflection curve shown in Figure 7.5, the critical load obtained by the computational method can be taken as the one where the curve becomes horizontal just before drooping down (at displacement 0.1 approximately).

7.2.2 Snap through phenomenon in a shallow arch

Snap through phenomenon is a unstable behavior of a structure under loading. It is a situation where load parameter decreases with an increase in displacement. This phenomenon is shown in Figure 5.1(a). A shallow arch model shown in Figure 7.6, is taken for the analysis. A central load is applied at the

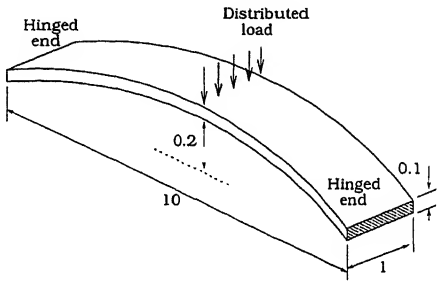

Figure 7.6: Model used for analysis of snap-through behavior

middle of the arch and corresponding load-deflection curve is shown in Figure 7.7. The cylindrical arc-length method is able to capture the snap-through behavior, but the conventional FEM solution is not. Rather, shown by dashed line, it almost jumps through the drooping portion of the curve as shown

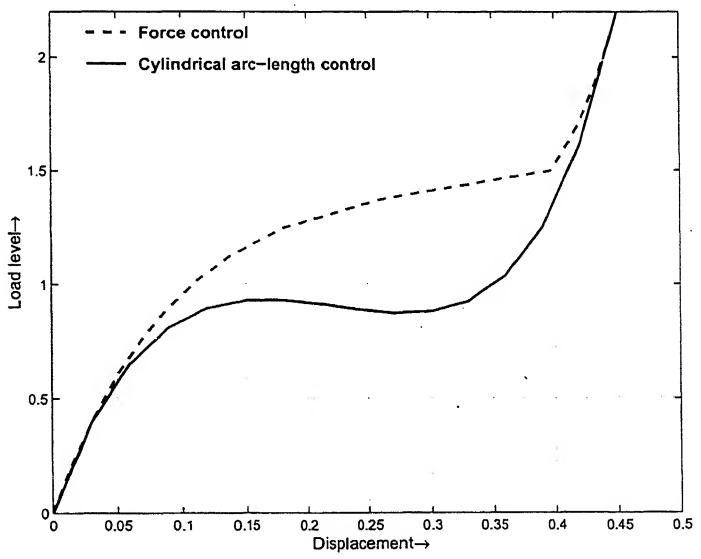

Figure 7.7: Comparison of cylindrical arc-length method with conventional solution method for snap-through phenomenon in a shallow arch

schematically in Figure 5.1(a). But here, the curve resulting from conventional FE solution lies some-

ANSYS results are generated using displacement boundary constraints at those nodes are close to the values obtained by the program.
The deformed shape along with the undeformed edges of the model used is shown in Figure 7.10.

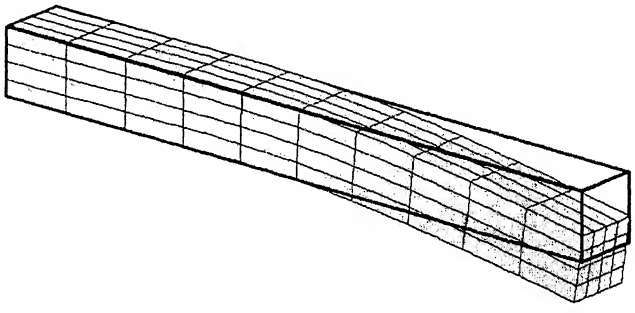

Figure 7.10: Deformed shape and undeformed edges from static contact analysis

7.4 Dynamic analysis

For dynamic analysis, the differential equation in time is discretized using Nemark-β algorithm. Initially the trapezoidal version of Newmark algorithm is used.

7.4.1 Bending analysis - stability of Newmark method

Newmark-β method with $\alpha = 0.25$ and $\delta = 0.5$ is applied for the beam model under flexure loading as shown in Section 7.1.1 with zero initial conditions. The results obtained are shown in Table 7.7.

End load	ANSYS result	Program with 5 UL steps	Program with 10 UL steps	Program with 15 UL steps
10 units	$2.4029\ e^{-2}$	$2.3958\ e^{-2}$	$2.6067\ e^{-2}$	$2.0019\ e^{-2}$

Table 7.7: End deflection for a beam under flexure load - dynamic analysis

These results, when plotted as load-displacement curves (Figure 7.11), an oscillation is observed in the solution. The oscillation is more for UL steps with smaller time step lengths. This oscillation is

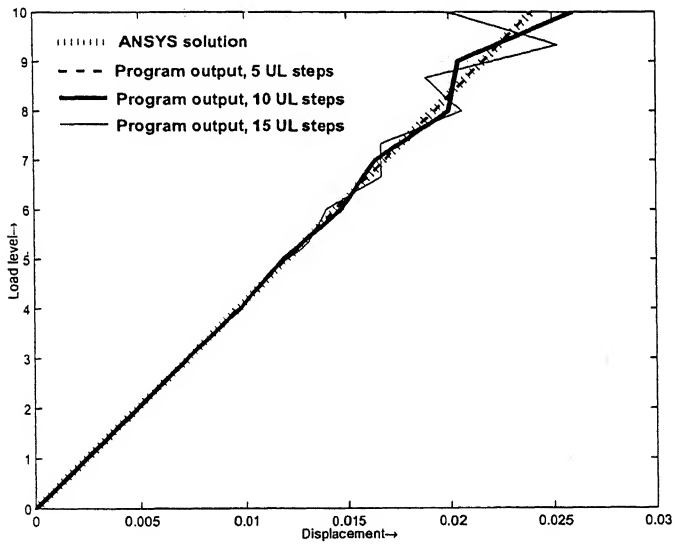

Figure 7.11: Increasing oscillations in Newmark-β technique with decreasing time step length using Newmark constants $\alpha = 0.25$ and $\delta = 0.5$ (trapezoidal rule)

seemingly because of the low values of the Newmark constants ($\alpha = 0.25$, $\delta = 0.5$) taken. The values of the Newmark constants, though mentioned as [13]

$$2\alpha \geq \delta \geq \frac{1}{2}$$

for unconditional stability, there remains some restrictions on the step lengths as seen in Figure 7.11. As suggested by Mahato, the numerical values of the Newmark constants are increased (to $\alpha = 1.56$ for $\delta = 2.0$, from the condition mentioned in Section 6.3) to get a stabilized load-displacement curve as shown in Figure 7.12.

This increment of the numerical values of the constants introduce algorithmic damping [13] to damp

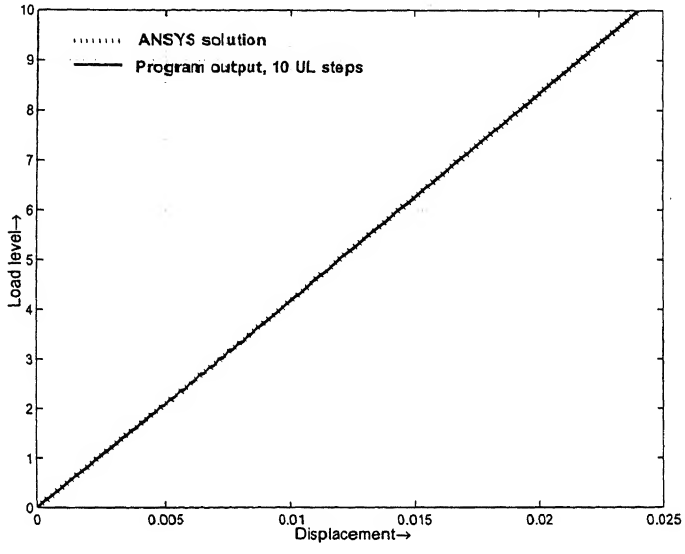

Figure 7.12: Stabilized Newmark-β method with algorithmic damping ($\alpha = 1.56$ and $\delta = 2.0$)

out the oscillations shown in Figure 7.11 and then, for conditional stability, some restriction on the time step lengths has to be imposed. This condition is given in Section 6.3.

7.4.2 Application of contact conditions

To damp out the oscillations in the solution, the values of the Newmark constants are kept as $\alpha = 1.56$ and $\delta = 2.0$ for dynamic analysis. With these values, the contact conditions are tested for the dynamic

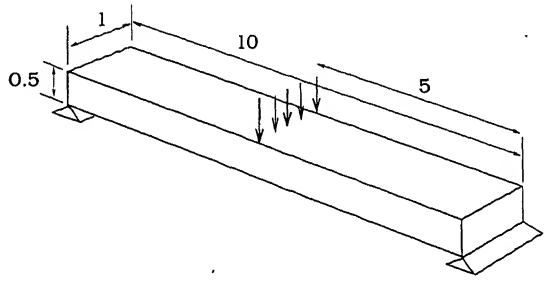

Figure 7.13: Model for analysis of dynamic contact

case for another model. The model is a beam, supported on hinges at two ends and loaded at the middle

as shown in Figure 7.13. The hinged joints are simulated by rigid contact for the corresponding nodes. A distributed force is applied on the middle line vertically downwards and corresponding displacement is computed.
The results are given in Table 7.8.

Load	ANSYS result	Program solution
10 units	$4.3434\ e^{-2}$	$5.0806\ e^{-2}$
20 units	0.08686	0.12541

Table 7.8: Mid point deflection of a hinged hinged beam - dynamic contact analysis

The results obtained from the code in this case, unlike the static contact analysis, is more flexible as compared to ANSYS. This is probably because of the algorithmic damping used by the increased numerical values of the Newmark constants. The deformed shape of the model is shown in Figure 7.14

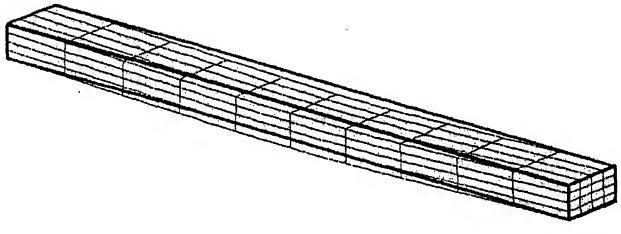

Figure 7.14: Deformed shape and undeformed edges from dynamic contact analysis

7.5 Thermoelastic deformation (dynamic analysis)

The model used for static analysis with axial force, is used for this case. One side of the bar is fixed and some force as well as heat flux is applied on the free end.
The results obtained from the program and ANSYS is listed in Table 7.9

End load	End heat flux	End deflection from ANSYS	End temp from ANSYS	End deflection from program	End temp from program
100	50	$4.958\ e^{-3}$	2545 K	$4.8161\ e^{-3}$	2517.43 K
200	50	$9.915\ e^{-3}$	2545 K	$9.6398\ e^{-3}$	2519.36 K

Table 7.9: Dynamic thermoelastic analysis

As the thermal analysis in ANSYS was carried out independently, the temperature for both the cases are same. The elastic response obtained from the simulation yet remains a little stiffer than ANSYS. For almost all the analyses simulated by the program is a little stiffer than the solution obtained through ANSYS. The existance of corner singularities in the models used may be responsible for that and a graded or adaptive mesh may be proposed for the accurate analysis of the structures.

Chapter 8

Conclusions and future scope

8.1 Conclusions regarding the present work

The target of the study is mainly to develop a formulation for the much discussed updated Lagrangian scheme. The basic definition of the method is used along with transformation laws from continuum mechanics along with proper approximation to get a honest incremental form of the UL method. In the literatures available, there are some small deformation assumptions plugged into the UL formulation. The general formulation without those approximations may be really useful for large strain-large rotation problems. Also the step size used in UL method becomes a parameter that one can control. With fewer assumptions, it is possible to increase the step sizes reducing the computational cost drastically. Thermodynamics is also included in the code to widen its possible scope of application.

In deducing the incremental form, objectivity of physical kinematic quantities are taken care of to make the analysis able to handle problems with large rigid rotation. Oldroyed rate, a general objective measure of stress rate is discussed, and the Jaumann-Zaremba rate form, a derivative of it and one of most popular stress rates, has been used in the computer program.

The contact formulation has been developed for both sticking and slipping contacts. The code is developed for only sticking contact with a rigid wall, but the Lagrangian multiplier technique is used in a flexible manner such that the frictional contact models and the two body contact problems can be modeled afterwards.

Some continuation techniques have been reviewed with the target to make the solution scheme more efficient. One of the continuation methods, the cylindrical arc-length method, has been plugged into the code to test the formulations used and a few global instable phenomenon have been captured.

After all, for the dynamic analysis, a problem regarding the oscillating nature of the solution from Newmark-β time integration scheme is faced. Some literatures have been referred regarding this issue, and following those, the oscillations had been damped out using algorithmic damping.

Finally, some standard models are used to validate the code. The problems, though very simple in nature, shows the scope of application of the code and its effectiveness. The numerical values obtained from it are compared with strength of material and/or ANSYS solution. The results obtained, expected to be a bit flexible than ANSYS, is not exactly satisfactory for all the cases. But they remain very close

to the bench-mark solution and ANSYS results.

8.2 Scope of further work

The idea behind developing the incremental updated Lagrangian method from the basics was mainly to get a general expression for the same without any pre-assumed points. This form seemingly can enable one to follow almost the actual path in solving a problem and the time steps of the solution procedure can be reduced. But as the current analysis is a linear one, the rejection of the higher order terms has put a limit on the number of UL steps used. A non-linear analysis and corresponding simulation may be carried out to focus on the reduction of the computational efforts.

The assumption discussed in Section 3.2, that the virtual displacement at time t and $t + \Delta t$ are same, is not always valid, specially for large displacement contact problems. The virtual displacement $\delta\tilde{u}$ itself, may be considered as a function of the space and time which will lead to a more general incremental weak form.

Also the application of the contact constraints has been a very restricted field in the present study. The present code may be extended to handle frictional contact and multi-body contact problems.

Among the continuation methods discussed, only the cylindrical arc length method has been successfully incorporated in to the computer program. But as mentioned in Section 5.4, this method is a crude one for predicting the correct load-displacement curve followed. The spherical as well as the linearized arc length methods may be included in the code and a comparative study may be carried out among them.

Another important issue regarding the set-backs of the simulation is the Newmark time integrator scheme used. Originally, trapezoidal scheme proposed by Newmark was used. Afterwards, the Newmark constants used have been modified (their numerical values increased) to stop the oscillations shown by the original scheme. This procedure seemingly induces algorithmic damping in the system. This may make the results to deviate from their actual values even though the spatial formulations have been carried out with precision. Some better time integration scheme should replace the Newmark one in the analysis.

Lastly, the possible issues, like corner singularities, causing the computational result to be a stiffer one though large strain and deformation has been considered, may be taken care of by a good meshing and solver algorithm. This will make the code a more dependable and robust one.

Bibliography

[1] Morton E. Gurtin. *An Introduction to Continuum Mechanics*. Academic Press Inc., 1981.

[2] Lawrence E. Malvern. *Introduction to the Mechanics of a Continuous Medium*. Prentice-Hall Inc., 1969.

[3] Klaus-Jürgen Bathe. *Finite Element Procedures*. Prentice-Hall, India, Seventh Indian reprint edition, 2003.

[4] Ted Belytschko, Wing Kam Liu, and Brian Moran. *Nonlinear Finite Elements for Continua and Structures*. John Wiley and Sons Ltd, 2000.

[5] Klaus-Jürgen Bathe, Ekkehard Ramm, and Edward L Wilson. Finite-element formulations for large deformation dynamic analysis. *Int. J. for Numerical Methods in Engg.*, 9:353–386, 1975.

[6] M.S. Gadala and J. Wang. ALE formulation and its application in solid mechanics. *Comput. Methods Appl. Mech. Engrg.*, 167:33–55, 1998.

[7] Harm Askes, Ellen Kuhl, and Paul Steinmann. An ALE formulation based on spatial and material settings of continuum mechanics. *Comput. Methods Appl. Mech. Engrg.*, 193:4223–4245, 2004.

[8] R.M. McMeeking and J.R. Rice. Finite-element formulations for problems of large elastic-plastic deformation. *Int. J. Solids Structures*, 11:601–616, 1975.

[9] M.A. Crisfield. *Non-linear Finite Elements Analysis for Solids and Structures (Volume-1: Essentials)*. John Wiley and Sons, 1991.

[10] M.A. Crisfield. *Non-linear Finite Elements Analysis for Solids and Structures (Volume-2: Advanced Topics)*. John Wiley and Sons, 1991.

[11] Peter Haupt. *Continuum Mechanics and Theory of Materials*. Springer, 1999.

[12] Article available in Division of Engineering, Brown University site (http://www.engin.brown.edu/courses/En222/Notes/FDplasticity/FDplasticity.htm).

[13] Robert D. Cook, David S. Malkus, Michael E. Plesha, and Robert J. Witt. *Concepts and Applications of Finite Elements Analysis*. John Wiley and Sons Inc., fourth edition, 2003.

[14] Jacob Lubliner. *Plasticity Theory*. Macmillan Publishing Company, 1990.

[15] Peter Wriggers. *Computational Contact Mechanics*. John Wiley and Sons Ltd., 2002.

[16] MEMON Bashir-Ahmed and SU Xiao-Zu. Arc-length technique for nonlinear finite element analysis. *Journal of Zhejiang University SCIENCE*, 5:618–628, 2004.

[17] Abhijit Mahato. Analysis of high speed impact of a ball with a plate. Master's thesis, IIT Kanpur, July, 2004.